PHILOSOPHICAL TRANSACTIONS OF THE ROYAL SOCIETY A MATHEMATICAL, PHYSICAL & ENGINEERING SCIENCES

The Electrical Resistivity of Gold Films

J. R. Sambles, K. C. Elsom and D. J. Jarvis

Phil. Trans. R. Soc. Lond. A 1982 **304**, 365-396
doi: 10.1098/rsta.1982.0016

Phil. Trans. R. Soc. Lond. A **304**, 365–396 (1982) [365]
Printed in Great Britain

THE ELECTRICAL RESISTIVITY OF GOLD FILMS

BY J. R. SAMBLES, K. C. ELSOM AND D. J. JARVIS
Department of Physics, University of Exeter, Exeter EX4 4QL, U.K.

(*Communicated by M. Blackman, F.R.S. – Received* 1 *May* 1981)

[Plates 1 and 2]

CONTENTS

 [Published 9 March 1982

We present measurements of the d.c. electrical resistance of three classes of pure epitaxial gold films in the thickness range 30 to 900 nm. The combination of diverse morphological techniques with temperature-dependent data from 2 to 300 K enables us to apply a new theory based on those of Mayadas and Shatzkes for grain-boundary scattering, and of Soffer for surface scattering. Gold, evaporated and annealed on mica substrates, produced ⟨111⟩ films which gave a mean microscopic surface roughness to Fermi wavelength ratio, r, of 0.05 and a grain-boundary reflexion coefficient, R_g, of 0.45. On KBr substrates, samples, prepared similarly, formed two distinct types of ⟨100⟩ film. Use of reflexion high energy electron diffraction and electron microscopy showed that the grain structure of these types of film differed; however, both gave an r of 0.1. An R_g of 0.10 was determined for one type but remained unknown for the other. Our results show how previous workers, often relying on the validity of Fuchs's theory and the misapplication thereof, have failed to present convincing evidence for specular surface scattering. We demonstrate the necessity for, experimentally, morphological observations and measurements over a wide temperature range, and, theoretically, the use of a method that combines the effects of both grain-boundary and angular-dependent surface scattering.

1. Introduction

There have been many studies of the effects of surface scattering on the resistivity of thin metal films. While most of the results suggest diffuse surface scattering, evidence from gold often indicates a high degree of specularity. This is a surprising result if one considers that the free electron Fermi wavelength in these metals, *ca.* 0.5 nm, is of the order of the nearest neighbour separation distance, 0.3 nm. Hence any missing atoms within the surface, adatoms on the surface or impurities at the surface constitute substantial roughness on the scale of the electron wavelength. It would appear, that to obtain a large degree of specularity, the metal surface should be atomically perfect and devoid of impurity species. Gold is one of the few metals that is both relatively easy to produce in epitaxial form and chemically inert. This leads to the possibility of an atomically flat surface. Hence, to attempt to study the influence upon resistivity of a highly specular metal surface, we have produced epitaxial gold films and measured their resistances from 2 to 300 K.

Several studies of the resistivities of gold films as a function of thickness are to be found in the literature. One of the earliest was that of Gillham *et al.* (1955). These authors prepared gold films by sputtering a thin layer on bismuth oxide or glass substrates. Some such samples were annealed at up to 200 °C when surface energy effects dominated annealing, and islands formed. To diminish the latter effect other films were produced coated with a second thin layer of bismuth oxide sputtered on to the top of the gold. These could then be annealed at up to 350 °C without substantial island formation. Subsequently they found that films could be annealed up to 450 °C with consequent further improvement in conductivity. They also performed resistance measurements on unannealed films at 293 K and 90 K which, on annealing at 350 °C, they remeasured at 472, 293 and 90 K. The data obtained on films ranging from 5.5 to 88 nm in thickness could be fitted to the following empirical expression for the thin-film resistivity, ρ_f,

$$\rho_f = \rho_\infty + k/t, \tag{1}$$

where ρ_∞ is the extrapolated infinite-thickness resistivity, t is the film thickness and k is a constant which was 0.57 fΩ m² for unannealed films and 0.066 fΩ m² for annealed films. The value of ρ_∞ varied markedly between the two types of sample; for example, at 90 K, ρ_∞

(unannealed) was determined to be 51 nΩ m whereas ρ_∞ (annealed) was 18.5 nΩ m. These values are both high, as were all ρ_∞-values in comparison with the accepted bulk resistivity value for gold at 90 K of 5.44 nΩ m (see for example Matula 1979). Having obtained this empirical expression they then equate it to the Fuchs (1938) relation for the resistivity of a film having a thickness much greater than the bulk electron mean free path, λ_∞. That is

$$\rho_f = \rho_\infty\left[1+\frac{3}{8}\frac{\lambda_\infty}{t}(1-p_F)\right], \tag{2}$$

where p_F is the specular component of electron reflexion at the film surface. Unfortunately they deduce $\lambda_\infty(1-p_F)$-values of 22.7 nm (20 °C unannealed) and 4.9 nm (20 °C annealed), concluding that λ_∞ is not less than 22.7 nm, which then does not satisfy the condition that $t \gg \lambda_\infty$. Hence their consequential deduction that p_F (20 °C annealed) is 0.88 is erroneous. It is far more likely that the correct explanation for their results rests with grain-boundary scattering. This not only substantially raises ρ_∞ in polycrystalline films but also gives a resistivity term which may be approximately proportional to $1/t$. The extent of the polycrystallinity was evident from electron diffraction studies of the annealed films. From these the authors conclude not only that 'the relative intensities of the various reflexions were not inconsistent with the random orientation of the gold crystallites' but also that 'the half breadths of the gold rings gave an approximate value of 4 nm for the dimensions of the gold particles in the plane of the film'. Presumably the unannealed films have even smaller grains. Hence we are forced to conclude that from this early set of data which is often quoted as evidence for specularity in gold films no such conclusion may be drawn, the results being dominated by grain-boundary scattering.

The early study discussed was followed by that of Ennos (1957) who both evaporated and sputtered gold on to various oxides and antimony sulphide. He found, as did Gillham *et al.*, that the resistivity of the films varied substantially with heat treatment. Samples were found to have the lowest resistivity on annealing at 350 °C. He quotes, that at 20 °C, 'at 20 nm, the resistivity is identical, within experimental error, with the bulk value'. From the data presented in the report, of the resistivity of gold on bismuth oxide, it is clear that there is a thickness dependence of the resistivity, even of the annealed films. It was noticeable, however, that the resistivities measured at 20 °C were substantially lower than those measured by Gillham *et al.*, indicating much less grain-boundary scattering. Furthermore, taking Ennos's value of λ_∞ of 62 nm for gold at 20 °C we see that the thickest film, 220 nm, should have a much greater resistivity than that of the bulk unless the surface scattering is substantially specular. For the 11.0 nm film he gives a resistivity at 20 °C of 40 nΩ m. Using this value in Fuchs's thin film expression

$$\frac{\rho_\infty}{\rho_f} \approx \frac{3}{4}\frac{(1+p_F)}{(1-p_F)}\frac{t}{\lambda_\infty}\left[\ln\left(\frac{\lambda_\infty}{t}\right)+0.4228\right], \tag{3}$$

we find $p_F = 0.3$. This indicates that gold is indeed partially specular even at room temperature and in polycrystalline films. However, we must be very cautious of these results as the author states that 'the substrate materials which were found to enhance the conductivity of the overlying gold layer were oxides of antimony, indium, bismuth and lead' and it would appear possible that the conductivity of these films is in some way enhanced by perhaps partial decomposition of the oxide into the metal and oxygen of which it is composed. In particular the

PHILOSOPHICAL TRANSACTIONS OF THE ROYAL SOCIETY A MATHEMATICAL, PHYSICAL & ENGINEERING SCIENCES

author comments that this decomposition of the oxide on evaporation 'was more noticeable for the oxide of bismuth than for the other three'. One final point to note from this work is that below 6 nm thickness the resistivity rose rapidly and also the temperature coefficient of resistance (t.c.r.) became anomalous. Both of these effects are attributable to films of this thickness or less being discontinuous (see Elsom & Sambles 1981).

The first study of thin single-crystal films of gold appears to have been that of Chopra *et al.* (1963). These authors studied not only epitaxial films of gold on mica but also polycrystalline films of a similar nature to those of the earlier studies. Their polycrystalline films, produced by either sputtering on to glass at 20 °C or evaporating on to mica at 20 °C, yielded curves of a similar nature to those of Gillham *et al.* with a thickness dependence that appears to be of the form of equation (1) where again ρ_∞ is much greater than the accepted bulk value, suggesting once more a high degree of grain-boundary scattering. For the films sputtered onto mica at 20 °C the data appear to follow the Fuchs $p_F = 0$ curve down to a thickness of about 40 nm, with a λ_∞ of 50 nm. This implies that at this thickness some islandization of these particular films is occurring. In contrast the single-crystal films produced on mica by either sputtering or evaporation, with the substrate at 300 °C, yielded quite different behaviour with apparently thickness-independent resistivities above some limiting thickness. For evaporated films with the sample voltage being continuously monitored during deposition, above 60 nm in thickness, the resistivity was constant at 30 nΩ m, 5.6 nΩ m greater than that for bulk gold but nevertheless apparently independent of sample thickness. The sputtered films in which the voltage was continuously monitored gave a constant resistivity of *ca.* 26 nΩ m above 40 nm, whereas with the measuring voltage interrupted the resistance appeared constant above 25 nm. There is a simple explanation for this difference in behaviour in that the applied voltage affects the nucleation kinetics: with no voltage the islands are connected more quickly than with a voltage present. From the thickness-independence of the resistivity, from above some fairly low limit, the authors conclude that at their measuring temperature, 20 °C for the cold substrate, the samples are specular. However, it is not clear if 300 °C was the measuring temperature for the epitaxial films or, since they compare the data at room temperature, whether the samples were cooled to 20 °C measured and then reheated to 300 °C. The authors state that 'the resistance of the films usually was measured continuously during deposition'. This would imply that the bulk resistivity to be compared with is that of gold at 300 °C. Furthermore, their thickness measurements which were based on the assumption that the evaporation rate was constant during any deposition relied on subsequent weighing of large-area substrates. Also the interpretation that the observation of a constant resistivity above a certain thickness is due to specularity is almost certainly false. The likely explanation is that, as we record in this work, the growth of the film changes its behaviour above a certain thickness. Initially the films are epitaxial and flat, but beyond a certain thickness they become polycrystalline with grain size no longer increasing as the thickness increases. Consequently the resistivity, dominated now by grain-boundary scattering, remains constant independent of thickness, but high with respect to the expected bulk value. This type of growth sequence has been recorded elsewhere, particularly for sputtered films (see, for example, Tellier & Tosser 1976). Thus one is forced to conclude that although the thickness-independence of the resistivity purports to show specularity there are some serious doubts about the significance of these often quoted results.

In the same year as Chopra *et al.* made the experiments described, Abelès & Thèye (1963)

performed some rather original experiments by depositing gold on to silica in 10^{-6} Torr† and subsequently annealing for 3 h at 150 °C. They then measured the electrical resistance and the optical constants of the film (anomalous skin effect). From these results they proceed to deduce that ρ_∞ is 23 nΩ m (20 °C), λ_∞ is 36 nm and $p_F \leqslant 0.47$. However, it is important to realize that their analysis is erroneous since they have not used the correct form for the anomalous skin effect in thin films; only more recently has this problem been solved (see Mayadas *et al.* 1972). Further, the influence of grain-boundary scattering is not considered and hence we must regard the interpretation of their results as dubious.

Some apparently definitive evidence that surface scattering in gold is certainly not diffuse comes from the work of Lucas (1964). He prepared 'specular' films of gold by both evaporation and sputtering on to bismuth oxide substrates. All were coated with a further layer of evaporated gold, and four-probe resistivity measurements were made at 26 ± 3 °C. For these films, as the surface layer was deposited, the resistance first rose and then fell. This would appear to be clear evidence for stating that the resistivity of the gold film has increased by the deposition of an unannealed layer on the top of a film and hence deducing that the surface has become significantly more diffuse as a consequence of this overlayer. Nevertheless, the author concludes his report by stating that 'much larger increases of resistance have been observed for superimposed layers of Pb, Sn, Fe, Al, Ag, Cr, SiO and Bi_2O_3 in place of Au. However, resistance increases have also been seen when either Bi_2O_3 or Pb was deposited upon non-specular Au films and so far it has *not been possible* to isolate the surface effect from other possible effects caused by alloying, the formation of inter-metallic compounds, or other as yet unknown mechanisms'. It is thus clear that the author himself is in some doubt as to the significance of his results so we look to further evidence for specularity in gold. This work was to an extent repeated by Chopra & Randlett (1967) who obtain the same type of results but interpret the resistance increase as being due to an extra mechanism. Meyer (1968) also studied this problem and came to the very interesting conclusion that gold films absorb gases when annealed at high temperatures so producing a surface phase that is then specular to conduction electrons. The deposition of a further layer of gold merely reduces this specularity. A further study of this nature is presented by Lucas (1971) who also gives a theoretical analysis of the double-layer problem.

Another of the more significant studies of gold films is that by Chopra & Bobb (1964) who deposited, by both evaporation and sputtering, gold films on to niobium oxide and mica substrates. Once again the technique for thickness measurement depended upon weighing a large-area sample after deposition. In this series of experiments the authors also measured the t.c.r. over a limited temperature range by using liquid nitrogen cooling. For the ordinary resistivity results, as before, the unannealed samples showed apparently diffuse scattering of the conduction electrons and for the niobium oxide substrates at 20 °C, a substantially increased thick-limit resistivity above the accepted bulk value, suggesting once again that the results are dominated by grain-boundary scattering. However, the resistivity of epitaxial films appears to be independent of thickness, at room temperature that is, for thicknesses greater than 40 nm but, as in the earlier study by Chopra *et al.*, it is higher than the accepted bulk value. Again the authors interpret these results as suggestive of a large specularity in gold: they deduce that p_F is 0.8. Further in this paper they present some strong substantiating evidence.

† Torr ≈ 133.322 Pa.

Both the resistivity ratio R_{298}/R_{78} and the t.c.r. are measured and show clearly for films from 50 to 500 nm in thickness that the resistive scattering of electrons in epitaxial gold is not totally diffuse, the data falling below the Fuchs totally-diffuse scattering limit. In contrast the films of gold sputtered on to mica fit very well Fuchs's theory for diffuse surface scattering. This work is the most significant study up to 1964 to show beyond any doubt that epitaxial films deposited on to mica give partially specular surface scattering. This work was also the first to attempt a low temperature study of these thin films. It was followed by Broquet & Nguyen Van (1967) who measured the resistivity from 54 to 300 K of gold films deposited in 5×10^{-8} Torr on to glass substrates. This was the first systematic study of the temperature dependence of gold films, albeit essentially polycrystalline ones. The films studied ranged from 18 to 69 nm in thickness. The authors concluded that the effective specularity p_F for these annealed polycrystal films ranged from zero to perhaps unity (although this value the authors themselves query) with a most common value of *ca.* 0.6. It is interesting to note that they determine the sample thickness by using the temperature dependence of the resistance, $\mathrm{d}R/\mathrm{d}T$, via

$$t = \frac{l}{w} \frac{\mathrm{d}\rho_\infty/\mathrm{d}T}{\mathrm{d}R/\mathrm{d}T}, \tag{4}$$

where l is the length between potential contacts, w is the sample width and $\mathrm{d}\rho_\infty/\mathrm{d}T$ is the temperature dependence of the bulk resistivity. For the thicknesses used, this, as we shall see later, may be a dubious procedure. Furthermore, like several of the previous studies, the results are almost certainly dominated by grain-boundary scattering.

Kadereit (1967) presents one of the most accomplished pieces of work to date. He studied polycrystalline gold films of thickness 50 to 600 nm deposited by evaporation on to glass substrates in various controlled vacua. The films were annealed for 45 min at 270 °C, grain size being substantially increased and the effect of grain-boundary scattering limited. Measurements at room temperature agree excellently with Fuchs's thick-film limit expression (2) with p_F equal to zero and a $\rho_\infty\lambda_\infty$ of 0.92 ± 0.02 fΩ m^2. If one uses the free-electron $\rho_\infty\lambda_\infty$-value it is found that p_F has to be negative, a physically unreasonable condition. Using the 4.2 K measurements and the thin sample limit of Fuchs's expression, Kadereit once more found excellent agreement, with, for the same samples, a lower $\rho_\infty\lambda_\infty$. If one takes the two sets of data and supposes that at room temperature p_F is zero and $\rho_\infty\lambda_\infty$ is 0.92 ± 0.02 fΩ m^2, then at 4.2 K the effective $\rho_\infty\lambda_\infty$ has decreased to 0.81 ± 0.01 fΩ m^2. Kadereit interprets this by suggesting that the number of conduction electrons per unit volume in gold is a function of temperature. In contrast he could have supposed that at low temperatures the gold films become more specular, in which case the thin-film expression (3) yields $p_F = 0.06$, it being assumed that $p_F = 0$ at room temperature. Such a temperature dependence of $\rho_\infty\lambda_\infty$ or p_F is a consequence of using Fuchs's theory and not the more exact theory due to Soffer (1967) as discussed by Sambles & Elsom (1980).

Namba (1968) evaporated gold films on to mica substrates held at either 20 or 100 °C in a vacuum of 2×10^{-6} Torr. Unfortunately, although his results show a substantial thickness dependence of resistivity, because he does not quote his ρ_∞-values, it is impossible to assess fully the significance of his data. They definitely show an enhancement in resistivity above that predicted by Fuchs's theory which is almost certainly attributable to percolation as the islandized films become discontinuous. His results have been re-analysed by Elsom and Sambles

PHILOSOPHICAL TRANSACTIONS OF THE ROYAL SOCIETY A MATHEMATICAL, PHYSICAL & ENGINEERING SCIENCES

who deduced an apparent specularity of 0.65 which is certainly a lower estimate since grain-boundary scattering may only further increase the resistivity on decrease in thickness.

The first work on the complete temperature dependence of the resistivity was by Jacobs *et al.* (1969) who investigated this dependence over the range 4.2 to 300 K. The thickness range investigated was, however, limited and results from only three films are quoted, these having thicknesses 130, 298 and 353 nm. The values for the specularity parameter for these films were 0.52, 0.82 and 0.95 respectively. They acknowledge the importance of grain-boundary scattering but did not attempt any analysis with this in mind. The variation of p from sample to sample as given is almost certainly a consequence of this omission.

Polycrystalline films on glass were studied by Reale (1970). He measured, at room temperature, the resistance of films from 10 to 100 nm in thickness. However, he fitted his data to theoretical values computed from Fuchs's theory using a λ_∞ of 36.5 nm and, we deduce, a bulk resistivity of 23 nΩ m. This bulk value was chosen to fit his experimental thick-sample resistivity which is higher than the accepted value, again caused by grain-boundary scattering. Nevertheless, it is clear that he does see a thickness dependence of conductivity which may be attributed either to surface or grain-boundary scattering, the grain size varying with film thickness. Hence, whether any credence can be put upon his estimate of $p_F \approx 0.2$ is a matter of some debate.

Another study that purports to show that p_F is not zero is that of Abelès & Nguyen Van (1970). These authors measured the resistivity of gold films less than 200 nm thick deposited in 10^{-8} Torr on to glass substrates. Analysing their results using Fuchs's theory they show that the free-electron value of $\rho_\infty \lambda_\infty$ is acceptable. This leads to a specularity p_F, lying between 0.3 and 0.5 which, although independent of temperature, is apparently a function of sample thickness. One of the most interesting aspects of this work is that they measure their sample thicknesses using X-ray interference between reflexion from the top and bottom surfaces.

Hubin & Gouault (1972) also studied, *in situ*, evaporated thin films of gold on silica substrates in u.h.v. Analysing their results using Fuchs's theory they obtain from a best fit to their data taken between 173 and 373 K, a $\rho_\infty \lambda_\infty$ of 0.863 ± 0.005 fΩ m^2 and a specularity of 0.6. The same results are presented with slightly more detail by Hubin & Gouault (1974).

Chauvineau & Pariset (1973) deposited, by evaporation, gold on to glass substrates in u.h.v. Their annealed film data, analysed using Fuchs's theory, yield a specularity of *ca.* 0.7, the accepted bulk resistivity value being assumed. All the films showed enhanced bulk resistivity which, once again, is attributed to grain-boundary scattering. Consequently their value of p_F is almost certainly an underestimate since the grain-boundary scattering can only decrease with the increase in grain size on increasing the film thickness.

Another study on glass as well as NaCl single-crystal substrates is that by Adamov *et al.* (1974), who produced films by both evaporation and sputtering. Like several of the other workers their thin samples had resistivities much greater than predicted by conventional surface scattering theories. This is caused by the islandization of their well annealed films, giving percolation in the poorly connected samples and thus a greatly enhanced resistance as shown by Elsom and Sambles. One further point from their results is that, apart from the sputtered films, the well annealed samples showed enhanced bulk resistivities implying once again significant grain-boundary scattering.

Golmayo & Sacedon (1976*a*), like Jacobs *et al.*, studied the temperature dependence of gold film resistivities down to 4.2 K. These authors deposited, by electron beam evaporation, 10 to

150 nm thick polycrystalline gold films on to glass; the films were not subsequently annealed. The results obtained are odd in two respects. Firstly, both the t.c.r. and the temperature dependence of the resistivity vary substantially between films, and secondly, there are some very strange 'kinks' in the resistivity data at about 40 K. They analyse the results, not using Fuchs's theory, but rather, more correctly, using Volger's (1950) grain-boundary scattering theory. In a second paper Golmayo & Sacedon (1976*b*) report results on the measurement of the Hall coefficients over the same temperature range but again they came to no conclusions about surface scattering.

Another different study of the resistivity of gold films is that by Heras & Mola (1976) who examined the annealing kinetics of thin polycrystalline gold films produced by evaporation on to glass substrates in 10^{-10} Torr. From their results on both annealed and unannealed samples a very clear thickness dependence is apparent for measurements at both 273 and 77 K. They do not analyse this data using Fuchs's theory since, like Golmayo & Sacedon, they are correctly concerned with the substantial grain-boundary scattering present in their films.

The most recent data on the resistivity of gold films is that of Cornely & Ali (1978), who deposited gold films on to glass using r.f. bias-diode and triode sputtering. They measured ρ_f at only 200 and 297 K and found, on analysing the thickness dependence using Fuchs's theory with $\rho_\infty \lambda_\infty = 0.840\ \mathrm{f\Omega\ m^2}$, that the specularity was zero for two of the samples and 0.62 and 0.74 for the others. The two with $p_F = 0$ were produced with higher bias voltage and possibly reflected a much rougher surface as a consequence of this bias. It is much more likely, however, that these films simply had smaller grains, the resistivity once more being dominated by grain-boundary scattering.

From the above review there is substantial evidence to suggest that gold films produced on room temperature substrates have 'bulk' resistivities that are significantly enhanced by grain-boundary scattering. Chauvineau & Croce (1968) have studied the influence of grain-boundary scattering in thin gold films and find that the reflexion coefficient for electrons striking a grain boundary is high, being about 0.6. With such a high reflexion coefficient we must expect polycrystalline films to be dominated by grain-boundary scattering, changes in resistivity with thickness being related merely to grain size. We see in several of the results thickness-independence of resistivity above a certain minimum thickness implying not that the surface scattering is largely specular but rather that the grain size, in these particular samples, does not increase with thickness beyond a certain maximum value. Further, the explanation of the apparent fit to Fuchs's theory of some of the data also lies with grain-boundary scattering. It is well known that grain size increases linearly with film thickness; this consequently gives a resistivity that has the $1/t$-dependence needed to appear to fit the commonly used approximation to Fuchs's theory, equation (2). Given this type of dependence, with p_F and $\rho_\infty \lambda_\infty$ as adjustable parameters, the data are easily, and wrongly, fitted to this theory. Hence we may, in general, conclude that virtually all of the above studies on polycrystalline films are worthless as regards their measurement of surface scattering.

Turning our attention to films which are annealed or produced at high temperatures we find most of the results show only a small increase of resistivity with decrease in thickness down to a certain thickness below which a rapid increase occurs. These observations are interpreted to imply either a relatively specular surface with little grain-boundary scattering or almost totally specular surface scattering with grain-boundary scattering dominating. The enhancement in the resistivity at low thickness indicates islandization and percolation conduction as

discussed by Elsom and Sambles. Unfortunately those studies that are not limited too seriously by grain-boundary scattering are very limited in number particularly as regards epitaxial films. Furthermore, even when such studies have been undertaken the results have been fitted to Fuchs's surface scattering theory with the incorporation of an angularly independent specularity parameter. No authors have attempted to analyse their data using a combination of grain-boundary scattering theory, which can rarely be neglected, and Soffer's surface scattering theory which incorporates an angularly-dependent specularity parameter.

Finally we note that almost no work has been undertaken on the temperature dependence down to 2 K of well prepared, epitaxial films. The aim of this work, of which we have already published a brief preview (Sambles *et al.* 1979), was not only to amend this situation but also to clarify the roles of both grain-boundary and surface scattering in thin gold films. In particular our aim was to determine the surface roughness by studying annealed, epitaxial films, and to ascertain whether gold is as specular as has been claimed in the past.

Notation

a	r.m.s. surface roughness
A	coefficient defined in $\rho = AT^N$
A_{ee}	electron–electron scattering parameter
A_f	film area
C	thin film limit of D/t
d	film mass density
D	grain size (mean)
D_∞	thick limit of D
e	electronic charge
G	Mayadas & Shatzkes grain-boundary function, defined by (9)
H	Mayadas & Shatzkes function defined by (16)
J_n	Debye integral defined by (18)
l	film length (between potential contacts)
l_e	effective film length
m_f	film mass
N	single effective power law exponent
p_F	Fuchs specularity parameter
p_S	Soffer specularity parameter
r	$= a/\lambda_e$
R	film resistance
R_g	grain-boundary reflexion coefficient
$\bar{R}_g$	mean R_g for polycrystalline film
R_{120}	film resistance at 120 K
R_{273}	film resistance at 273.16 K
S	defined by (6)
S_{Fs}	Fermi surface area
t	film thickness (general)
t_e	effective film thickness
t_i	film thickness according to interferometric measurements
t_m	$= m_f/A_f d$

t_r	resistance thickness given by (21)
t_0	D_∞/c
t_1	underlayer thickness
t_2	overlayer thickness
T	temperature
u	$= \cos\theta$
w	film width
w_e	effective film width
α	Mayadas & Shatzkes grain-boundary parameter
α_∞	$= \alpha$ at infinite film thickness
β	$= \alpha_\infty/\lambda_\infty$
θ	angle of incidence of electron at surface w.r.t. surface normal
Θ	Debye temperature for phonon scattering
κ	$= t/\lambda_\infty$
λ_e	conduction electron Fermi wavelength
λ_i	impurity limit of λ_∞
$\lambda_{g\infty}$	$= \rho_\infty\lambda_\infty/\rho_{g\infty}$
λ_∞	bulk mean free path
ρ	resistivity (experimental)
ρ'	normalization constant from (17)
ρ_f	experimental film resistivity
ρ_{fF}	film resistivity from Fuchs's theory
ρ_{fS}	film resistivity from Soffer's theory
ρ_g	grain-boundary enhanced resistivity
$\rho_{g\infty}$	grain-boundary resistivity for infinitely thick samples
ρ_i	impurity resistivity, bulk residual resistivity
ρ_p	phonon resistivity
ρ_1	underlayer resistivity
ρ_2	overlayer resistivity
ρ_3	resistivity at 3 K
ρ_{273}	resistivity at 273.16 K
ρ_∞	bulk resistivity
$\rho_{\infty,120}$	$= \rho_\infty$ at 120 K
$\rho_{\infty,273}$	$= \rho_\infty$ at 273.16 K
σ_∞	$= 1/\rho_\infty$
ϕ	azimuthal angle of incidence of electron at surface

2. Theory

(a) *Surface scattering*

It is apparent that a study of the nature presented here requires a theory that combines grain-boundary scattering with an appropriate model of surface scattering. In the past, experimentalists have used primarily Fuchs's surface scattering theory to analyse their data. Sambles and Elsom have already shown that this theory, based upon a specularity parameter which is independent of angle of incidence of the electrons, may only be used as an approxi-

mation in the thick sample or very rough surface limits. Since, in this study, we are concerned with thin samples and, further, anticipate that surfaces will be relatively smooth, we have chosen to use the more exact theory due to Soffer. He extended the work of Ziman (1960), introducing, in the limit of no lateral surface correlation, a specularity parameter p_S that depends on the angle of incidence θ, measured from the surface normal, taking the form

$$p_S(\cos\theta) = \exp[-(4\pi r)^2\cos^2\theta], \tag{5}$$

where $r = a/\lambda_e$, a being the r.m.s. surface roughness and λ_e the Fermi wavelength. Using appropriate boundary conditions Soffer then solved the linear Boltzmann equation for a metal slab. Defining

$$S(\kappa, p, u) = 3(u-u^3)(1-p)(1-e^{-\kappa/u})/2(1-pe^{-\kappa/u})\kappa, \tag{6}$$

where $\kappa = t/\lambda_\infty$, and $u = \cos\theta$, t being the mean sample thickness and λ_∞ the bulk mean free path, we find the familiar Fuchs equation for thin-film resistivity ρ_{fF} takes the form

$$\frac{\rho_\infty}{\rho_{fF}} = 1 - \int_0^1 S(\kappa, p_F, u)\,du, \tag{7}$$

where p_F is the Fuchs specularity and ρ_∞ is the resistivity due to impurities and phonons. Similarly with the use of p_S, Soffer's theory gives

$$\frac{\rho_\infty}{\rho_{fS}} = 1 - \int_0^1 S(\kappa, p_S(u), u)\,du. \tag{8}$$

This expression has been evaluated and compared with existing data on aluminium by Sambles and Elsom who show clearly its advantages over Fuchs's theory. However equation (8) does not apply to metal samples in which there is substantial grain-boundary scattering. It is essential that Soffer's approach be combined with an appropriate grain-boundary scattering model to provide suitable theoretical comparisons with our data.

(*b*) *Grain-boundary scattering*

Several theories have appeared that attempt to predict the influence of grain-boundary scattering upon the resistivity of thin films. The most commonly used is that due to Mayadas *et al.* (1969) who discuss a model of a film that represents the grain boundaries as parallel partially reflecting planes, perpendicular both to the E field and to the plane of the sample and placed an average distance D apart. For specular reflexion at the sample surface ($p_F = 1$, or $r = 0$) Mayadas *et al.* obtain, for the grain-boundary enhanced resistivity, ρ_g,

$$\rho_\infty/\rho_g = 1 - \tfrac{3}{2}\alpha + 3\alpha^2 - 3\alpha^3\ln(1+\alpha^{-1}) = G(\alpha), \tag{9}$$

where

$$\alpha = \frac{\lambda_\infty}{D}\left(\frac{R_g}{1-R_g}\right), \tag{10}$$

D being identified with the mean grain width and R_g the reflexion coefficient for electrons striking the grain boundary. To examine the influence of this grain-boundary scattering as a function of film thickness it is necessary to model the functional dependence of the mean grain width on sample thickness. In the thin-film limit D is found to vary linearly with t, but, in

general, as the film thickness increases a limiting grain size D_∞ is reached. To account for this we have chosen to approximate the grain size dependence upon thickness by

$$\frac{1}{D} = \frac{1}{D_\infty} + \frac{1}{Ct} = \frac{1}{D_\infty}\left(1 + \frac{t_0}{t}\right), \tag{11}$$

where C is a constant that often lies in the range 0.5 to 5; the second form containing $t_0 = D_\infty/C$ is a slightly more convenient form and is used in the analysis. Combining expressions (11) and (9) one can predict the thickness-dependent grain-boundary contribution to the resistivity of a thin sample. In the high temperature limit, that is small λ_∞,

$$\frac{\rho_\infty}{\rho_g} = 1 - \frac{3}{2}\frac{\lambda_\infty}{Ct}\left(\frac{R_g}{1-R_g}\right). \tag{12}$$

This can be rearranged to give, for a film whose resistivity is dominated by grain-boundary scattering,

$$\rho_g = \rho_\infty\left[1 + \frac{3}{8}\frac{\lambda_\infty}{t}\frac{4R_g}{C(1-R_g)}\right]. \tag{13}$$

It is transparently obvious from this expression why, in the past, Fuchs's approximate expression (2) has been used to fit thin-film data when, in reality, (13) should be used. If we make the reasonable supposition that $C = 2$ for many of the polycrystalline studies reviewed in the Introduction, then we find that, with a p_F of 0.7, this is equivalent to an R_g of 0.13, an eminently acceptable value. We further find, by re-examining the appropriate limit of expression (11), that at high temperatures, for thick-film samples

$$\rho_g = \rho_\infty\left[1 + \frac{3}{8}\frac{\lambda_\infty}{D_\infty}\left(\frac{4R_g}{1-R_g}\right)\right]. \tag{14}$$

This gives a simple expression for the enhancement of the resistivity of thick-film samples at room temperatures. Often we find D_∞ is limited to less than 20 nm while λ_∞ is of the same order (α still being small because R_g is small, the validity of the approximation being retained). This then gives an enhancement of ρ_f over ρ_∞ of *ca.* 25%, typical of the magnitudes observed in practice. In general, of course, simple expressions like (13) and (14) are not valid since they pertain only to the small-α limit and furthermore they do not incorporate any contribution from surface scattering. Hence the final task of theory is to combine this model with that of Soffer to incorporate, as one, both grain-boundary and surface scattering.

(*c*) *Grain-boundary and surface scattering*

Mayadas & Shatzkes (1970) have used a combination of Fuchs's theory and (9) to derive an expression for the total resistivity of a thin film. We have followed the same approach to combine Soffer's surface scattering model with the same grain-boundary expression to give

$$\frac{\rho_\infty}{\rho_f} = G(\alpha) - \frac{4}{\pi}\int_0^{\frac{1}{2}\pi}\int_0^1 \frac{\cos^2\phi}{H(u,\phi)}\, S(\kappa H(u,\phi), p_s(u), u)\, \mathrm{d}u\, \mathrm{d}\phi \tag{15}$$

where

$$H(u,\phi) = 1 + \alpha/[(1-u^2)^{\frac{1}{2}}\cos\phi]. \tag{16}$$

Note that the grain size, D, brought into Soffer's expressions (8) through H, via α, acts primarily as a modification to the mean free path reducing the surface contribution from the infinitely large grain case. Until recently, progress with the above type of expression has been

limited, but with the introduction of highly efficient methods of numerical integration such expressions are now readily computed.

It is apparent on examination of (15) that ρ_f relies on a knowledge of several parameters, including r, R_g, D_∞, t_0, λ_∞ and ρ_∞. The object of the present study is to obtain values for R_g, D_∞, t_0 and, in particular, r. However, to proceed to this goal it is necessary to have reasonable values for the bulk parameters ρ_∞ and λ_∞.

(*d*) *The bulk resistivity*

A number of scattering mechanisms will contribute to the bulk resistivity. In particular we are concerned in these samples with phonon scattering and, at low temperatures, impurity scattering. The assumptions made for this analysis are that the impurity scattering introduces a temperature-independent contribution ρ_i and that the phonon contribution, ρ_p, is well approximated by the Bloch–Gruneisen formula (see Ziman)

$$\rho_p = \rho' \left(\frac{T}{\Theta}\right)^5 J_5\left(\frac{\Theta}{T}\right), \tag{17}$$

where Θ is the Debye temperature associated with phonon scattering, being of the order 160 K, $J_n(x)$ is the Debye integral given by

$$J_n(x) = \int_0^x \frac{z^n e^z \, dz}{(e^z - 1)^2}, \tag{18}$$

and ρ' is a constant chosen to make the ice point resistivity, ρ_{273}, some accepted value. This then gives

$$\rho_\infty = \rho_i + \rho_p. \tag{19}$$

There are various arguments to suggest that (17) is a particularly poor approximation to the resistivity of a metal such as gold whose Fermi surface makes contact with the Brillouin zone boundary. Also Kaveh & Wiser (1980*a*, *b*) have given details of possible deviations from the validity of (19) but we can assume that these may be small by comparison with the grain-boundary and surface terms. A justification for the use of both (19) and (17) is that our thickest samples give results that accord very well with these two approximations. Similar behaviour has already been recorded in aluminium by Sambles *et al.* (1981). Therefore, while accepting that several of the assumptions involved in the Bloch–Gruneisen derivation are untenable for gold, nevertheless the form of the predicted temperature-dependent resistivity would appear to be substantially correct.

There is, however, one other contribution to the bulk resistivity that might be expected to manifest itself, if only weakly. It is now accepted that electron–electron scattering will add to the resistivity a term of the form $A_{ee} T^2$. MacDonald (1980) has recently estimated that A_{ee} has a magnitude of 3.0 fΩ m K^{-2}. From this we find that the electron–electron contribution at 20 K will only be about 1.2 pΩ m which can therefore be neglected by comparison with the phonon resistivity at 20 K which is *ca.* 200 pΩ m. Below 20 K the film resistivity become residual and hence this term may be ignored.

From the above considerations, and with suitable fitting to the thicker film data, it is possible to obtain a form for the bulk resistivity and it only remains necessary to find the bulk mean free path to be able to evaluate fully expression (15).

(e) *The bulk mean free path*

In the free electron approximation the product of the bulk mean free path λ_∞, with the bulk resistivity ρ_∞, is a constant which for gold takes the value 0.84 fΩ m^2. This does not take into account in any way the features of the Fermi surface brought about by contact with the walls of the first Brillouin zone. From de Haas–van Alphen measurements this reduces the Fermi surface area by approximately 7%. Hence we deduce, from the approximate expression for the conductivity

$$\sigma_\infty = 1/\rho_\infty = (e^2/12\pi^3\hbar)\,\lambda_\infty S_{\mathrm{Fs}}, \tag{20}$$

where S_{Fs} is the Fermi surface area, that $\rho_\infty\lambda_\infty$ is increased to 0.90 fΩ m^2. However one cannot ignore Kaveh & Wiser's argument that those electrons near the Brillouin zone boundary have a very short phonon scattering time, and so contribute little to the conductivity. This implies that while σ_∞ is little modified by these electrons, λ_∞ is in effect increased as the significant electrons will be the ones with the longer mean free paths. Thus although the necks appear to increase the Fermi surface area, the ineffectiveness of those electrons in the vicinity of the necks results in a further apparent reduction in Fermi surface area. We have consequently used a $\rho_\infty\lambda_\infty$-value of 0.96 f$\Omega$ m^2. Fortunately, as it later materializes, it is not necessary to know this parameter with precision and the change in fitting the theory to the data brought about by the possible range of $\rho_\infty\lambda_\infty$ is less than the precision to which we can define the parameters r, R_{g} ,etc.

3. Experimental

(a) *Preparation of evaporated films*

The gold used in this study was 99.9999% pure (supplied by Johnson–Matthey Ltd). It took the form of fine powder which was easily mounted into a tungsten basket-filament from which it could subsequently be evaporated. All evaporations were performed in an oil-pumped system operating at a pressure of *ca.* 10^{-4} Pa. Two types of substrate were used, freshly cleaved mica to produce $\langle 111\rangle$ films and freshly cleaved potassium bromide to give $\langle 100\rangle$ films. In both cases the substrates were first heated for half an hour at approximately 20 °C above the temperature at which deposition occurred. They were then cooled to 280 °C for mica and 390 °C for KBr substrates and evaporation was begun. To ensure cleanliness of the films, several evaporations of the pure gold were performed in the system before the production of any of the measured samples to limit contamination arising from impurities in the tungsten filament and from alien atoms sputtered off the walls and contents of the evaporation chamber. It was found that epitaxial films were formed on both substrates by using an initial slow rate of deposition of about 5 nm min^{-1} for 20 nm, followed by an increase to *ca.* 40 nm min^{-1} until the necessary thickness had been deposited. Both deposition rate and approximate film thickness were monitored by means of a quartz crystal oscillator. After deposition the films were annealed for half an hour just above the deposition temperature before being slowly cooled to room temperature.

The samples so produced had two configurations. Thick samples were rectangles approximately 40×5 mm^2 in size. However, thin samples, to which it was almost impossible to make direct electrical contact mechanically, had, predeposited, four contact electrodes produced on the same substrate. These electrodes consisted of thick (more than 200 nm) layers, of the same

PHILOSOPHICAL TRANSACTIONS OF THE ROYAL SOCIETY A MATHEMATICAL, PHYSICAL & ENGINEERING SCIENCES

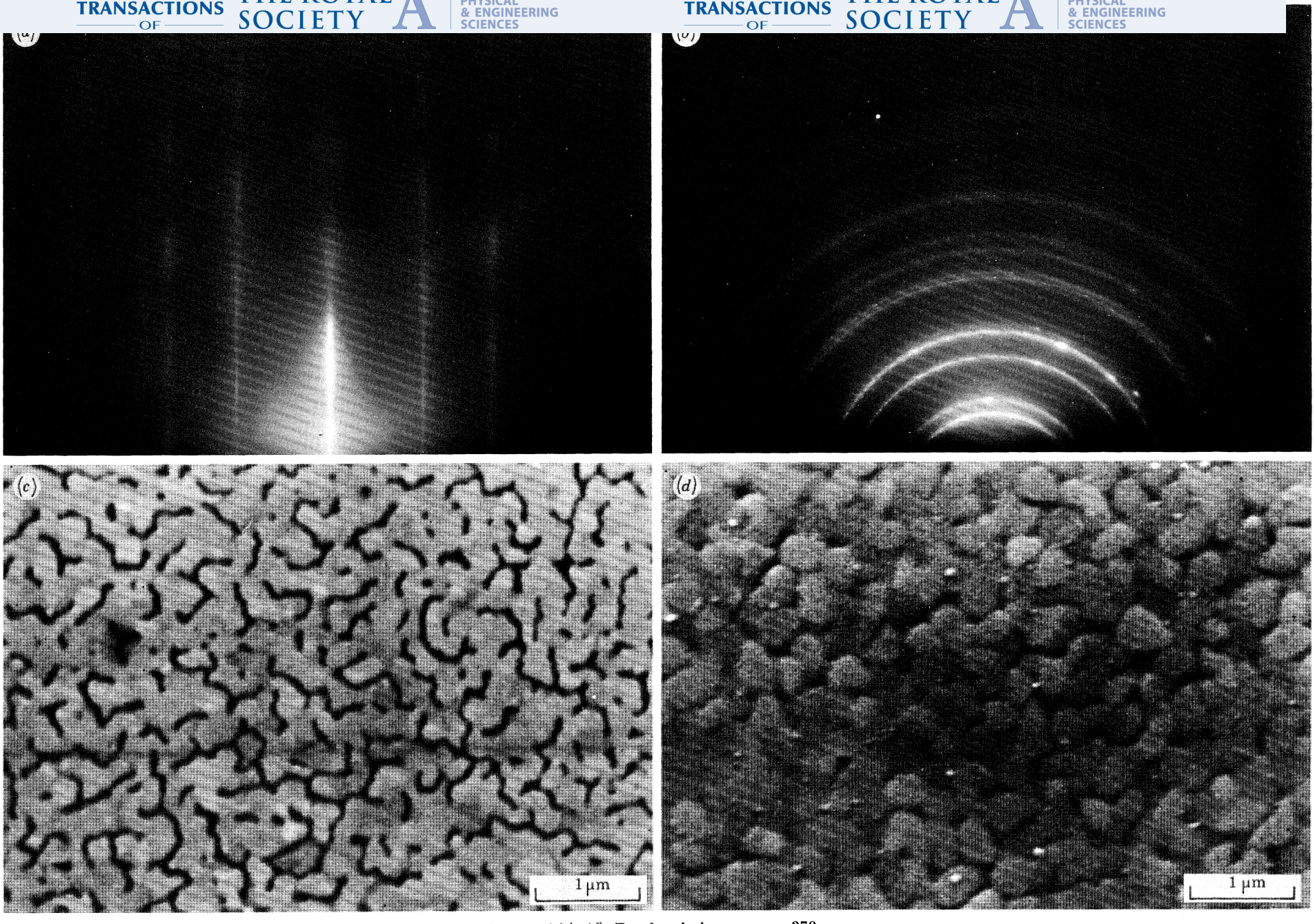

(*Facing p. 378*)

FIGURE 1 (*a*)–(*d*). For description see page 379.

PHILOSOPHICAL TRANSACTIONS OF THE ROYAL SOCIETY A MATHEMATICAL, PHYSICAL & ENGINEERING SCIENCES

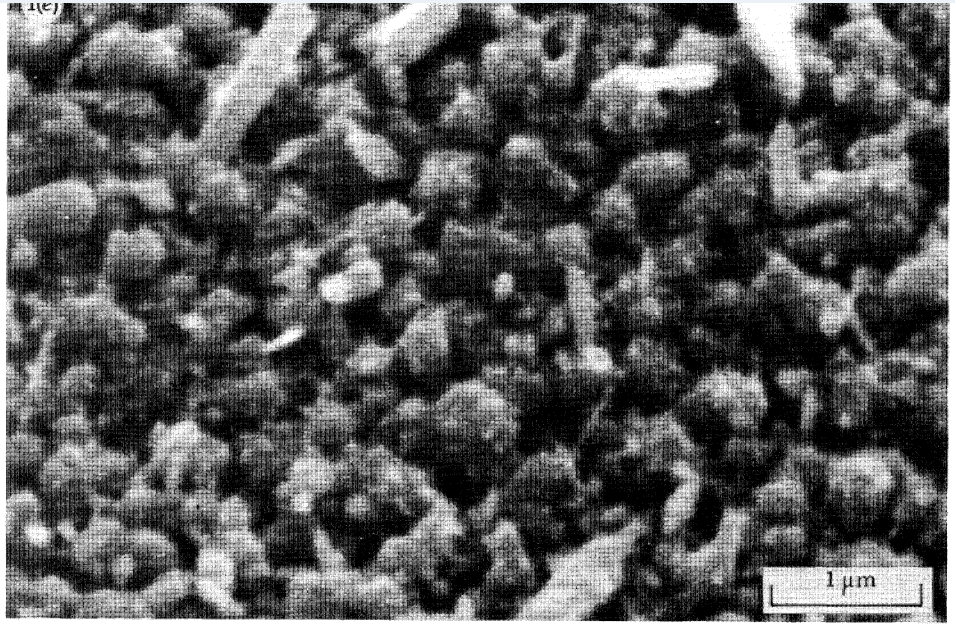

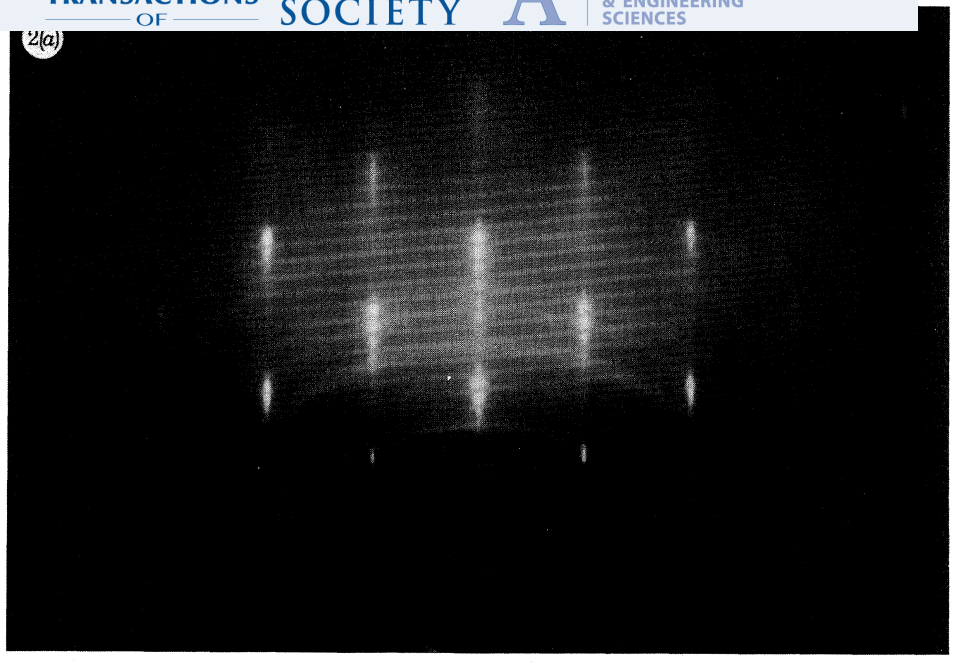

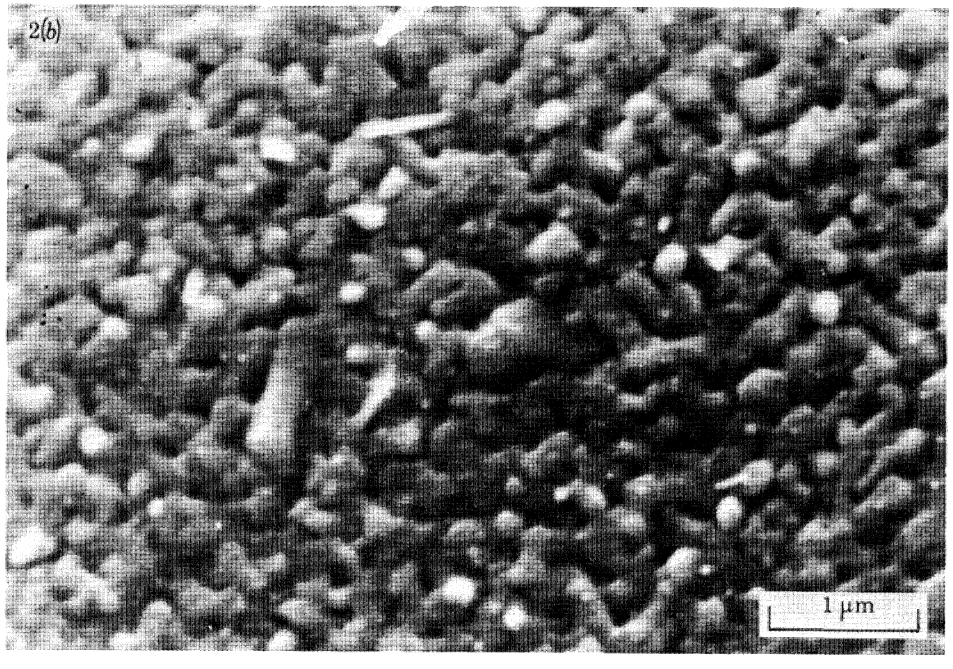

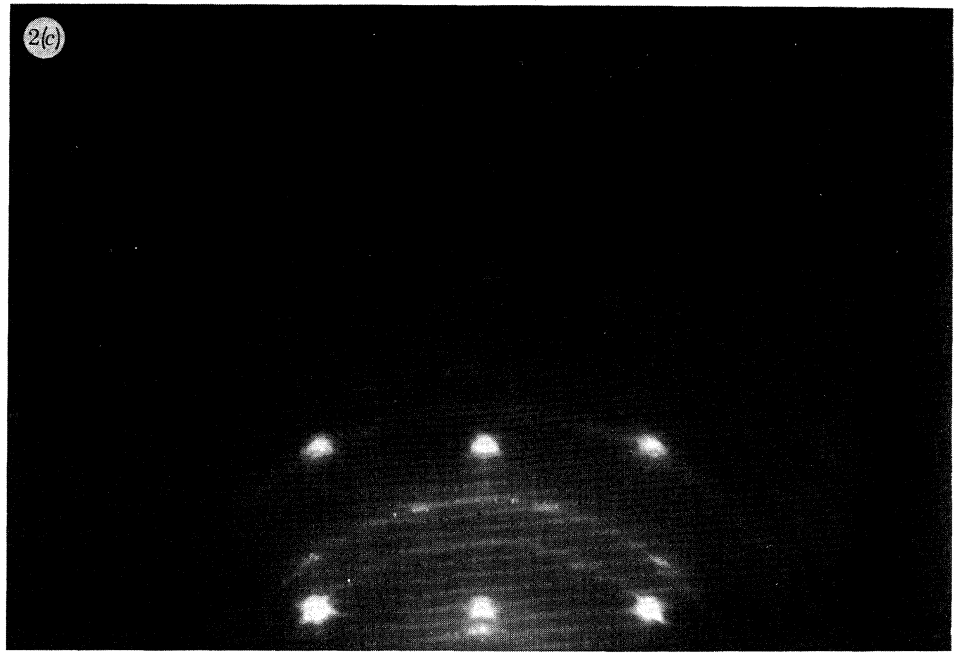

FIGURES 1 (*e*) and 2 (*a*)–(*c*). For description, see opposite

gold, deposited so that the voltage electrodes made point contact with the sides of the sample film while the current electrodes overlapped the ends of the film by a few millimetres. These thinner films were only 2 mm wide.

(*b*) *Morphology of evaporated films*

The samples were examined by X-ray diffraction, reflexion high energy electron diffraction (r.h.e.e.d.), scanning electron microscopy and transmission electron microscopy of carbon replicas. X-ray diffraction indicated that films were oriented with a ⟨111⟩ axis perpendicular to the mica substrate or with a ⟨100⟩ axis perpendicular to the KBr substrate. R.h.e.e.d., however, gave a somewhat different and much more informative picture. With mica the thin films produced very 'streaky' diffraction patterns (see figure 1*a*, plate 1). These patterns indicate that up to about 160 nm the gold films on mica are very flat and double-positioned. Above this thickness polycrystalline rings start to appear, until at 210 nm the 'streaks' have disappeared completely (see figure 1*b*). This indicates that thick gold films produced in this way have an epitaxial layer of *ca.* 160 nm upon which is a polycrystalline layer of appropriate thickness to give the total film thickness. Scanning electron micrographs also illustrate this very clearly. In figure 1*c* we show a micrograph of a channelled film that is just conducting. Figure 1*d* shows a flat film of *ca.* 120 nm thickness, while figure 1*e* (plate 2) is typical of the thick films having a superposed rough upper layer containing grains *ca.* 300 nm in diameter.

For the KBr samples a different picture emerges. None of the electron diffraction patterns were as 'streaky' as those produced from gold on mica indicating less macroscopic surface flatness. Moreover, nearly all the samples were to some extent polycrystalline as indicated by faint rings in the diffraction pattern. A typical pattern is shown in figure 2*a* (plate 2). It was discovered that these films did not become rough like the ⟨111⟩ films, only the very thick sample of 889 nm showing a similar behaviour to the thick ⟨111⟩ films. For comparison with the mica samples we show a good quality film in figure 2*b*. Another interesting feature of the electron diffraction patterns was the tendency for the ⟨100⟩ films to give diffraction 'stars' as illustrated in figure 2*c*. This is caused by the faceted nature of the grains.

A useful value that may be obtained from the electron micrographs is the ratio of mean grain size to film thickness. This parameter has great relevance later in the interpretation of the resistivity results in terms of grain-boundary scattering. For the ⟨111⟩ films it is found that for samples thicker than 50 nm and thinner than 160 nm the grain width is about three times the mean sample thickness. Beyond 160 nm the grains stop growing at a mean diameter of *ca.* 450 nm and it is at this stage that the rough overlayer starts to form. For thicknesses less than 50 nm the samples are partially discontinuous and in this case the mean mass thickness

---

Description of plates 1 and 2

Figure 1. (*a*) Reflexion electron diffraction pattern (40 kV) from a high quality ⟨111⟩ gold film on mica. Note the long 'streaks' and double positioning. (*b*) Reflexion electron diffraction pattern (40 kV) from a thick ⟨111⟩ gold film with a polycrystalline overlayer. (*c*) Scanning electron micrograph of a just-conducting ⟨111⟩ film on mica. Note the channelled structure. (*d*) Scanning electron micrograph of a flat ⟨111⟩ film on mica showing grain size. (*e*) Scanning electron micrograph of a thick ⟨111⟩ film on mica showing very rough overlayer.

Figure 2. (*a*) Reflexion electron diffraction pattern (40 kV) from a ⟨100⟩ gold film on KBr showing a mixture of rings from a thin overlayer plus short 'streaks' indicative of a stepped surface. (*b*) Scanning electron micrograph of a low r.r.r. ⟨100⟩ gold film on KBr showing the grain size. (*c*) Reflexion electron diffraction pattern (40 kV) from a ⟨100⟩ gold film showing faceted nature of grains as illustrated by diffraction 'stars'.

PHILOSOPHICAL TRANSACTIONS OF THE ROYAL SOCIETY A MATHEMATICAL, PHYSICAL & ENGINEERING SCIENCES

becomes less than the grain thickness as less of the substrate is covered with gold. Consequently the mean ratio of mass thickness to island width appears to decrease whereas in reality the grain-width to grain-thickness ratio probably remains close to 3:1. For the ⟨100⟩ films grown on KBr the results obtained from the electron micrographs show two types of film. One type is apparently quite rough, macroscopically, (see figure 2*b*) with a mean grain width of the order of half the film thickness, that is with grains substantially more rounded in comparison with the ⟨111⟩ platelets in mica. This also agrees with the r.h.e.e.d. evidence. There is, however, a second type of ⟨100⟩ film in which the film is merely stepped with no obvious granularity. Rather than being formed of a mosaic of grains the sample then appears to be almost a single crystal with steps and dislocations. This family of films have a grain width very much larger than the mean thickness although it is impossible to obtain from the micrographs a value for this ratio. Finally, we note that evidence from high resolution replicas and the electron diffraction patterns suggests that all the ⟨100⟩ films had a thin overlayer of well spaced polycrystalline islands about 10 nm in diameter.

Thus, summarizing the results of the morphology studies, we find that the films are largely well oriented ⟨111⟩ on mica or ⟨100⟩ on KBr. On mica the films are macroscopically very flat up to about 160 nm, with a mean grain width to thickness ratio of 3:1; beyond this thickness a very rough layer grows on top of the flat underlayer. For the ⟨100⟩ films on KBr two types of growth are apparent. Most films show substantial granularity with grain widths of the order of half the mean film thickness. In contrast a few of the ⟨100⟩ films appear to be almost single crystalline. All the ⟨100⟩ films have a dilute coverage of *ca.* 10 nm diameter islands of polycrystalline gold. Hence we may deduce the following. For the films grown on mica we expect to see very little surface scattering, the dominant mechanism being grain-boundary effects. Also above 200 nm in thickness the behaviour of the resistivity will change, while below 50 nm percolation conduction will be evident. For the ⟨100⟩ films grown on KBr we expect to see a similarly low amount of surface scattering, although the films are perhaps a little less flat atomically, with, in one set, a large amount of grain-boundary scattering, while for the single crystal samples we should expect little or no grain-boundary scattering. Precisely what effect the dilute overlayer of polycrystalline islands will have is unknown. Bearing these observations in mind we now turn our attention to the determination of the resistivities of these films as a function of temperature.

(*c*) *Measurement of the resistance*

After removal from the evaporation system the specimens were mounted into a conventional pumped-helium resistivity cryostat. Resistances were measured by using a standard four-probe technique, the sample voltage being monitored by a Keithley 180 D.V.M. capable of resolving 30 nV. Normally a current of 100 mA was used, but for the thinnest samples this was reduced to 10 mA to eliminate any significant heating of the sample. Using an automatic data-logging sequence the sample voltage and temperature (determined by use of a 0.03 % iron-doped gold–chromel thermocouple) were recorded from *ca.* 2 to 300 K. To avoid spurious thermal voltages, at each temperature, two voltage readings were taken, one with reversed current. Consequently, the mean eliminates any thermal e.m.fs. Further, the readings were taken over a long period involving a rate of change of sample temperature of less than 0.3 K min^{-1}. This ensures isothermality of readings while also minimizing thermal shock to the sample. The resistance data acquired in this fashion took the form of approximately 1000 pairs of data points for every

sample. This raw data which consisted of sets of readings of both sample voltage and thermocouple e.m.fs had then to be converted to resistivities and temperatures. The temperature was obtained from a calibration of the thermocouple achieved by replacing the sample with a standard rhodium–iron resistance thermometer. This gave a final temperature accuracy of better than ± 0.1 K at 10 K falling to a maximum inaccuracy of ± 0.2 K at 150 K. Data points having thus readily been obtained in the form of temperature against resistance, it is then straightforward to convert this to temperature against resistivity, provided one knows the sample thickness.

(*d*) *Determination of sample thickness*

Before detailed discussion it is relevant to specify what one means by sample thickness. Normally, the thickness of a film is defined as the *mean mass thickness*, t_m, given by

$$t_m = m_f/A_f d$$

where m_f is the mass of the film of area A_f and d is its density. This is not necessarily the same as the thickness determined by using a technique that does not measure, in some way, the mass of the film: it will only be the same if the films are flat and parallel-surfaced. Fortunately most films are parallel enough so that the error introduced by use of different techniques is not significant. However, one class of film fails completely in this respect, that is 'channelled' films (those that are not completely continuous). In this case the mass thickness is not the same as the thickness determined by resistance measurements or by interferometry, and it is with these very thin films that extra care must be taken in determining their 'correct' thickness.

One of the conventional methods for determining the mass thickness of an evaporated film is by use of a quartz crystal oscillator, the resonant frequency of which changes as the metal is deposited on it. Unfortunately this method relies on the assumption that the metal 'sticks' as well to the substrate (often at an elevated temperature) as it does to the quartz crystal. This is certainly not true for the early stages of deposition. Another method for determining the mass thickness is to hold the evaporation rate constant, the quartz crystal being used as a monitor, and to deposit a very thick layer over a long period of time. Then, by weighing, the rate of deposition per unit time is ascertained and so the thicknesses of the thinner films formed over a short period of deposition, at the same rate, is determined. Chopra *et al.* measured film thicknesses using this technique. Unfortunately, of course, in the thin-film limit this also fails because, once again, the initial condensation rate is substantially less than that finally achieved when the whole substrate is covered with the depositing metal.

Another technique that has often been used is that of interferometry but here the thickness measured, t_i, is very difficult to relate to t_m since it will depend significantly upon the manner in which the second metal layer nucleates on both the film and the bare substrate. In general t_i is likely to be greater than t_m. Because of the problems outlined above we attempted to determine the thickness of our films from the resistance of the samples themselves. This thickness is then yet a different quantity which we label t_r. It, like the other determinations is equal to t_m for large thicknesses. The definition of t_r that we use is that given by von Bassewitz & von Minnigerode (1964):

$$t_r = \frac{l}{w}\frac{(\rho_{\infty,273} - \rho_{\infty,120})}{(R_{273} - R_{120})}, \qquad (21)$$

PHILOSOPHICAL TRANSACTIONS OF THE ROYAL SOCIETY A MATHEMATICAL, PHYSICAL & ENGINEERING SCIENCES

where R_{273} is the resistance measured at 273.16 K and R_{120} is that at 120 K. The bulk resistivity at 273.16 K, $\rho_{\infty,273}$ was taken to be 20.1 nΩ m and that at 120 K, $\rho_{\infty,120}$ was taken to be 7.79 nΩ m (Meaden 1966). This technique is satisfactory in samples whose resistivity ratios are substantially greater than ten, in which case the difference in surface or grain-boundary terms between 120 K and 273 K causes an insignificant error in thickness. For samples with resistivity ratios less than ten it is possible that a temperature-dependent term arising from either surface or grain-boundary scattering will make $\rho_{273}-\rho_{120}$ different from $\rho_{\infty,273}-\rho_{\infty,120}$, and hence t_r as defined in (21) will not even be the correct resistivity thickness. Fortunately, as we see later, this is not the case for gold where the surface term is very small and where the grain-boundary contribution is largely temperature-independent. However, where this technique for determining t does fail, like all the others, is for 'channelled' films. Here the conduction is by means of percolation paths, and the effective film length, l_e, is greater than l, and its effective width w_e is less than w. Consequently from expression (21) the deduced thickness is always less than the mass thickness since $l_e/w_e > l/w$ causing $R_{273}-R_{120}$ to be bigger than expected. In contrast the effective resistivity thickness, t_e, is actually greater than t_m since only regions with metal present can conduct. Hence we have four thicknesses that concern us for these very thin films, t_r deduced from (21), t_m the mass thickness estimated from the quartz crystal oscillator, t_i from interferometric measurements and finally t_e, the effective resistivity thickness. They are related by $t_r < t_m < t_i < t_e$. Furthermore, unless one knows accurately the morphology of these films neither t_m nor t_e may be determined. Hence these particular films cannot be compared with theory, most theories using t_m as the thickness variable. For the rest of the samples t_r is totally satisfactory and is, to within a small percentage, the same as t_m. As a check, some of the thicker films were also measured by interferometry, and the two thicknesses t_r and t_i agreed to within the accuracy of determination.

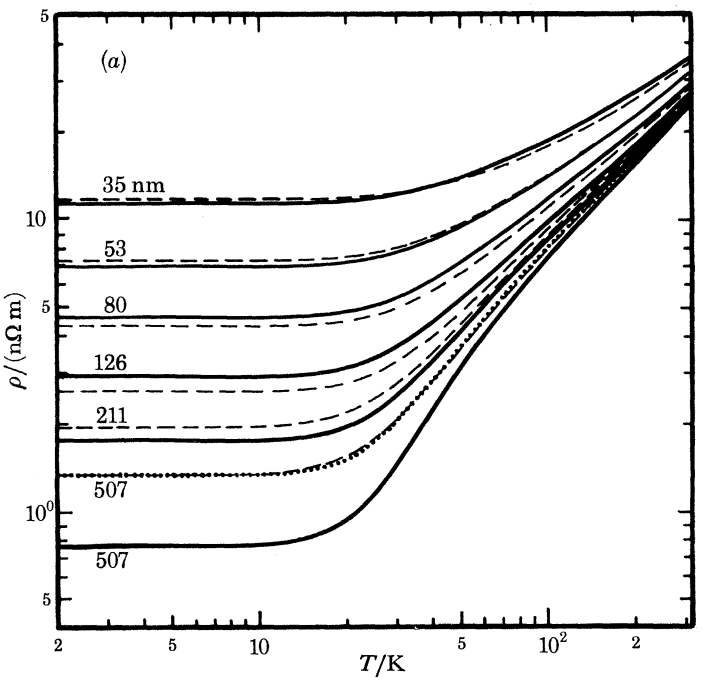

For description, see opposite.

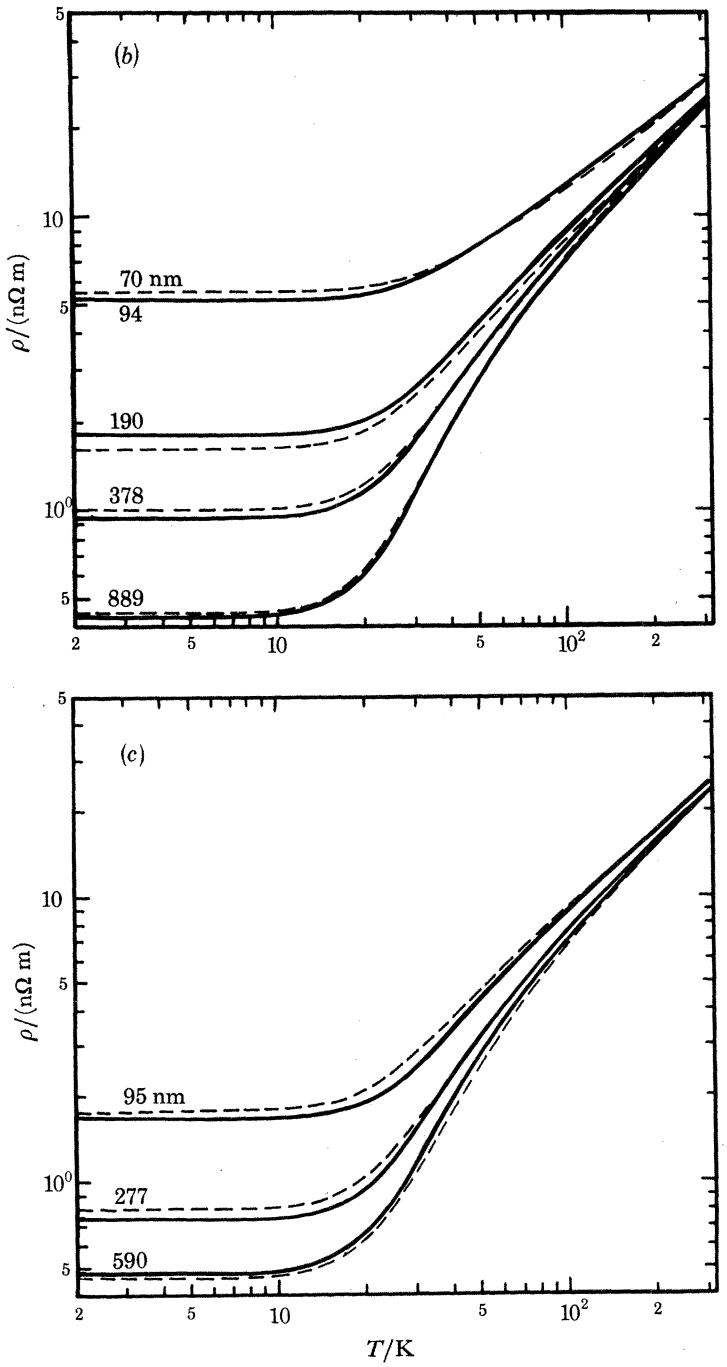

FIGURE 3. Resistivity, ρ, against temperature, T, on a double logarithmic scale for a few of the samples studied. Dashed lines are from experiment; full lines are the theoretical curves (see text). (*a*) ⟨111⟩ Gold on mica substrates. The dotted line is a theoretical curve fitted to the 507 nm sample only (The 35 nm sample had a t_r of *ca.* 20 nm. This can be shown by extrapolation of the theory on figure 5 to correspond to an effective thickness of 35 nm.) (*b*) ⟨100⟩ Gold on KBr substrates, small grains. (The 94 nm sample is fitted to a 70 nm theory which is the mean thickness of the two thinnest samples of this type, both of which had the same resistivity, see figure 5.) (*c*) ⟨100⟩ Gold on KBr substrates, large grains.

PHILOSOPHICAL TRANSACTIONS OF THE ROYAL SOCIETY A MATHEMATICAL, PHYSICAL & ENGINEERING SCIENCES

4. Resistivity results

(*a*) *The temperature dependence of the resistivity*

A selection of results, reduced to the form of resistivity against temperature, is presented in figure 3. The data, corrected for thermal contraction, are represented by the dashed lines, the density of data points (*ca.* 1000 per curve) being so high that individual points are not presented. Typical errors are less than the thickness of the dashed line. Inspection of these data shows three essential points. Firstly, all three sets have very similar temperature dependences; secondly, there are two distinct sets of ⟨100⟩ film data, the higher quality films having the higher resistivity ratios; and thirdly, the thicker ⟨100⟩ samples have much lower resistivities than the thicker ⟨111⟩ samples.

(*b*) *Residual removed resistivities*

It is impossible to obtain the resistivity at 0 K so, as a good approximation, we have taken the mean of the data around 3 K to define our residual resistivity. This may be expected to be higher by no more than about one part in 10^5 (the limit of measurement accuracy) than the true residual resistivity of these films. By removing this resistivity, ρ_3, from the data we obtain the temperature dependence of the resistivity. If the residual contribution is temperature dependent, so-called deviations from Matthiessen's rule will occur and we would expect the temperature dependences obtained by the above procedure to vary systematically with sample

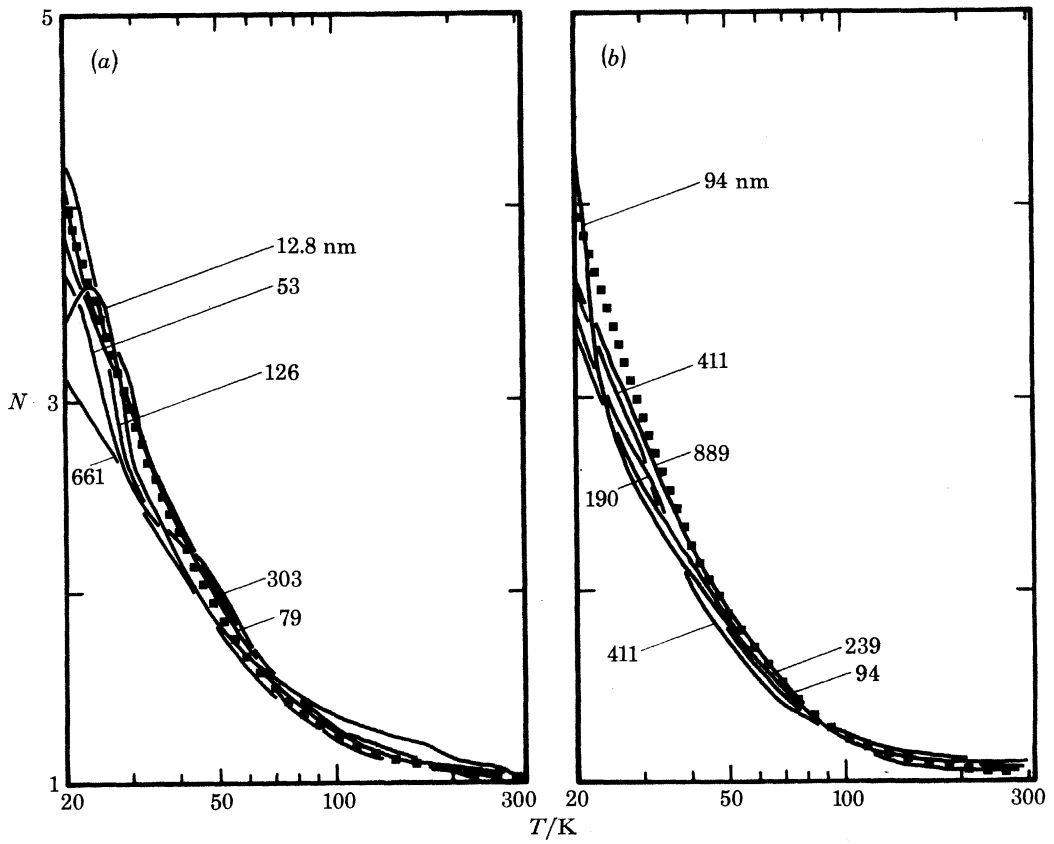

For description, see opposite.

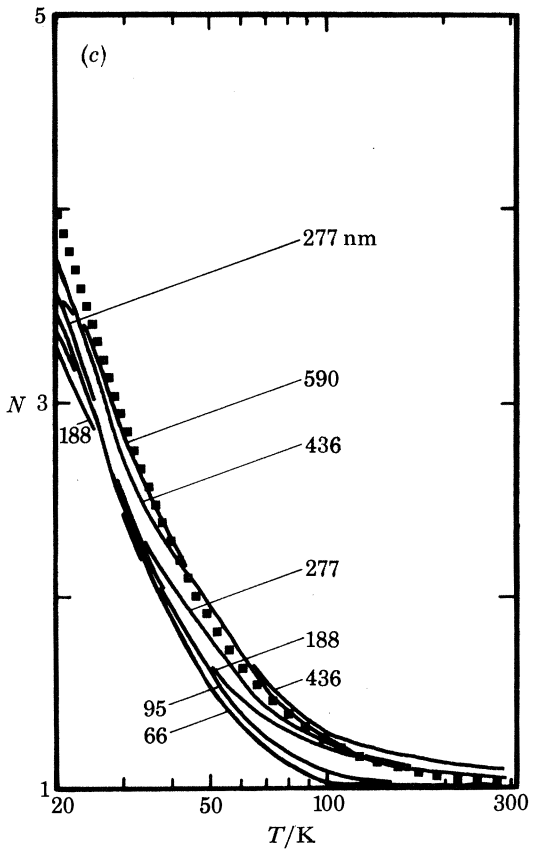

FIGURE 4. The coefficient N in the equation $\rho - \rho_3 = AT^N$ against T for some of the samples studied. The dotted curve is a Bloch–Gruneisen fit with $\Theta = 157$ K: (*a*) ⟨111⟩ gold on mica substrates; (*b*) ⟨100⟩ gold on KBr substrates, small grains; (*c*) ⟨100⟩ gold on KBr substrates, large grains.

thickness. Such a variation was sought by plotting the coefficient N as a function of temperature where we define N by

$$N = \mathrm{d}[\lg(\rho - \rho_3)]/\mathrm{d}(\lg T).$$

These graphs are presented in figure 4 for a representative set of samples. Clearly the ⟨111⟩ films and the low resistivity ratio ⟨100⟩ films show no systematic trends, all films having the same N-dependence with temperature in the region 20 to 300 K. However, the high resistivity ratio ⟨100⟩ films do show systematic deviations for the thinner films at higher temperatures. This suggests that these films will not fit so well a theory based on Mayadas & Shatzkes's grain-boundary scattering approach because this theory predicts only very small changes in the temperature dependence of N with thickness. As we see later, these films do not accord so well with this particular theory.

5. Analysis of the results

(*a*) *General*

As we discussed in §2, we have used a combination of Soffer's surface scattering theory and Mayadas & Shatzkes's grain-boundary scattering theory to provide comparisons with our data.

This combined theory needs, as outlined in §2(*d*) and 2(*e*), ρ_∞ as a fundamental parameter. To obtain ρ_∞ we have attempted a fit of the naïve Bloch–Gruneisen expression (17) to our thick-film data. This is best illustrated by examination of figure 4. Here the theoretical N-curve is produced from the Bloch–Gruneisen theory with a Θ of 157 K and an ice-point resistivity of 20.1 nΩ m (Meaden). The value of Θ was chosen to give the best fit to the high temperature thick-film data, 157 K lying very close to the accepted value of 162 K (Meaden). Inspection of figure 4 shows a trend for the experimental data to have lower N-values below 50 K than this simple theory predicts. This almost certainly illustrates that the general fit to Bloch–Gruneisen is fortuitous, a far more elaborate theory being necessary to give the correct N-dependence. However, these deviations are only significant in regard to the residual removed data and henceforth we turn our attention back to the original data where these deviations may be ignored. In this case we can use, to define ρ_∞, the Bloch–Gruneisen curve to give ρ_p together with an impurity contribution ρ_i. The total theory that we fit to our data is then based on the following parameters.

(*a*) ρ_i. The bulk residual resistivity. This is the first of the parameters that was allowed a significant range, falling within the limits corresponding to a residual resistivity ratio (r.r.r.) greater than 100 but less than 3000 (r.r.r. $= \rho_{273}/\rho_3$).

(*b*) $\rho_\infty\lambda_\infty$. This was chosen to be 0.96 fΩ m² as discussed in §2(*e*). Together with ρ_i and ρ_p this gives λ_∞.

(*c*) $\beta = D_\infty^{-1}R_g/(1-R_g)$. This contains both R_g and D_∞ as variable parameters. Since we had no prior knowledge of D_∞, β was largely unconstrained except in so far as $0 < R_g < 1$.

(*d*) $t_0 = D_\infty/C$. This was also unconstrained because as for β, D_∞ is unknown, but note that $\beta t_0 = C^{-1}R_g/(1-R_g)$ gives, with a knowledge of C, R_g.

(*e*) r. This parameter was initially unconstrained. However, it very soon became apparent that unless it was less than *ca.* 0.25 the predicted temperature dependences of ρ were quite different in character to those observed in practice (see §5(*c*, ii), figure 9).

To proceed further in terms of fitting the data to a theory containing several unconstrained variables we adopted the following approach. Firstly, ρ_i and r were constrained to values close to those expected, i.e. 0.04 nΩ m and 0.05 respectively, and a two-dimensional minimization was performed on β and t_0 to give the best fit of theory to the residual resistivity values. Then with these four parameters as starting points, a four-dimensional minimization was performed to give the overall best fit of theory to these residual data, so determining ρ_i, r, β and t_0. It was found, in general, that the fitting was dominated by t_0 and β, being largely independent of ρ_i and r provided these parameters were below certain limits, indicating that surface scattering has little influence on the resistivity of these films.

Following from this the standard way of comparing theory with experiment is to plot ρ/ρ_∞ against t_m/λ_∞ for various thicknesses and temperatures (λ_∞s). In our case this is apparently not possible because ρ_∞ is not known accurately. However, we can deduce a value for $\rho_{g\infty}$, that is the resistivity that an infinitely thick sample with grain-boundary scattering would have, from the above fit of the theoretical curves to the residual data. This residual $\rho_{g\infty}$ is given, from (9), by

$$\rho_i/\rho_{g\infty} = G(\alpha_\infty)$$

where

$$\alpha_\infty = \lambda_i\beta,$$

λ_i being the impurity-dominated bulk mean free path. The resistivity $\rho_{g\infty}$ at any other temperature is found from the appropriate modification to the above expressions by adding the phonon, Bloch–Gruneisen, contribution to the resistivity and so calculating the mean free path. It is then simple to produce plots of $\rho/\rho_{g\infty}$ against $t_m/\lambda_{g\infty}$ where $\lambda_{g\infty} = \rho_\infty \lambda_\infty / \rho_{g\infty}$.

(*b*) *Films on mica substrates*

As already discussed the ⟨111⟩ films show three distinct regions of growth. Films less than 50 nm in thickness are channelled, between 50 and 160 nm they are continuous and very smooth, while above 160 nm a very rough polycrystalline overlayer forms. Thus any simple thickness-dependent analysis involving surface and grain-boundary scattering has to be restricted to the films whose thicknesses lie in the central region. These films are expected to have substantial grain-boundary scattering due largely to double positioning, and minimal surface scattering due to their very flat surfaces. The best fit to the residual resistivity of these films is shown by the continuous curve in figure 5. We determined that $r \approx 0.05$ implying a

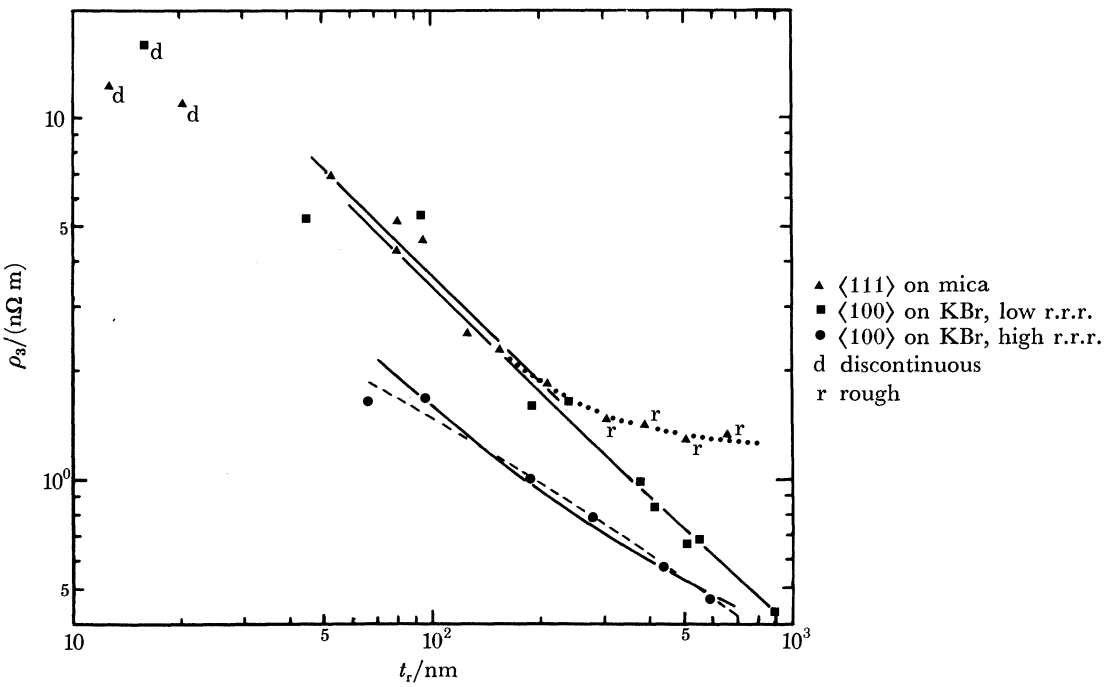

FIGURE 5. Residual resistivities as a function of thickness for all films studied. Full lines are theoretical curves (see text). The dotted line is a theoretical fit to the thick mica samples while the dashed line is a theoretical fit, with surface scattering only, to the large-grained ⟨100⟩ films.

high degree of surface flatness. The bulk resistivity ratio was found to be greater than 500 with *ca.* 1000 giving the optimum fit, this value lying well within the expected range. The parameter β was found to be 0.03 μm^{-1} and t_0 had a best value of 8.7 μm. These two parameters are eminently reasonable and, given a ratio of mean grain diameter to film thickness, C, of three, we deduce a reflexion coefficient at the grain boundaries, R_g, of the order of 0.45, a D_∞ of *ca.* 25 μm being used. This large value of D_∞ effectively makes D proportional to t over the whole of this thickness range, hence giving a resistivity which, as a first approximation, varies as $1/t$.

This explains why so many authors have used the approximate expression (2) for Fuchs's surface scattering theory, which gives such a $1/t$-dependence, to analyse their thin-film data and hence have ascribed to the surface that which in reality is a grain-boundary effect.

The fitting procedure described works only for the data that lie in the thickness range 50 to 160 nm. For the thinner samples the apparent resistivity thickness, t_r, is, as discussed above, much less than the effective thickness and so the data points are well to the left of this curve. In contrast the thicker samples have a resistance that arises from two components. There is a contribution from the smooth underlayer, approximately 160 nm thick, with a parallel contribution from the very rough overlayer. Thus we have

$$\frac{1}{R} = \frac{w}{l}\left(\frac{t_1}{\rho_1}+\frac{t_2}{\rho_2}\right),$$

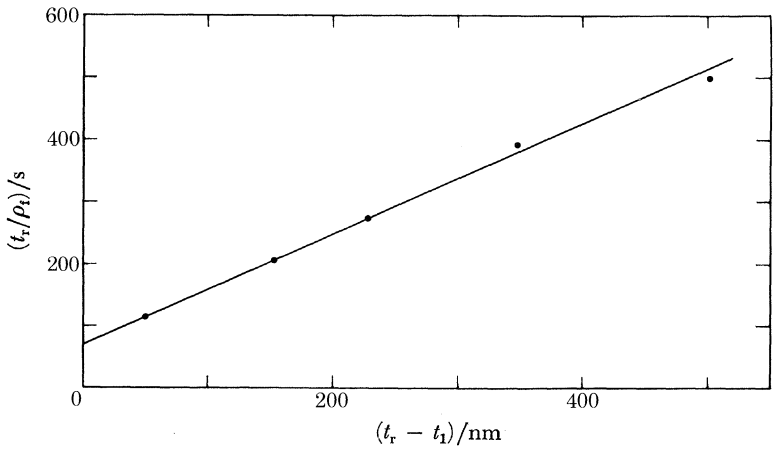

FIGURE 6. Plot of thickness divided by resistivity against overlayer thickness for the thick ⟨111⟩ gold films on mica.

where the flat layer of thickness t_1, has resistivity ρ_1, and the overlayer has thickness t_2 and resistivity ρ_2. Assuming that ρ_2 varies little with t_2, as a first-order approximation we find

$$\frac{t_r}{\rho_f} = \frac{t_1}{\rho_1}+\frac{t_r - t_1}{\rho_2}.$$

Hence t_r/ρ_f against $t_r - t_1$ is a straight line of slope $1/\rho_2$ and intercept t_1/ρ_1. A graph of this nature is presented in figure 6 where an excellent fit is observed, with $\rho_2 = 1.12\ \text{n}\Omega\ \text{m}$, $\rho_1 = 2.20\ \text{n}\Omega\ \text{m}$ and $t_1 = 160$ nm. This theory also provides the dotted fit to the thick ⟨111⟩ film data in figure 5. Notice the ρ_2-value corresponds to the resistivity that a film of thickness 340 nm would have were it flat. This implies an equivalent grain size, no surface scattering in the rough layer being assumed, of order 1.3 μm. This is about five times the size of the grains in the overlayer and shows that the grain-boundary scattering parameter, $\bar{R}_g$, between polycrystals in the overlayer is substantially lower than that in the ⟨111⟩ film between double-positioned (d.p.) islands. One can estimate that

$$[\bar{\bar{R}}_g/(1-\bar{R}_g)]_{\text{poly}} \approx \tfrac{1}{5}[R_g/(1-R_g)]_{\text{d.p.}}.$$

This gives, for the polycrystalline overlayer, which inevitably contains some double positioning, an $\bar{R}_g$ value of 0.15. From this, we may deduce that, since the ⟨100⟩ films will not be

double-positioned, their grain-boundary reflexion coefficient is likely to be less than but close to $\bar{R}_g$.

Putting this analysis of the rough overlayer together with the interpretation of the flat $\langle 111 \rangle$ films we have a satisfactory explanation of the residual resistivities of the gold-on-mica films. Now we turn our attention to the temperature dependence of the resistivity of the films lying in the thickness range 50 to 200 nm. We present data for all such films over the whole temperature range in figure 7*a*. Now the variable parameters, ρ_i, r, β and t_0, have been chosen to give the best fit over the whole range. Full lines are the theoretical curves produced from expression (15). The best fit is given by the same parameters as for the residual data. These same parameters are used to produce the theoretical curves (full lines) of figure 3*a*. From the thicker samples in figure 3*a* it is apparent that the theoretical curves fall well below the experimental values. To illustrate, nevertheless, that these thicker samples fit the same sort of analysis but with a modified β and t_0 we have adjusted these two parameters accordingly to fit the 507 nm sample. In this case the dotted curve is the theory, and apart from a small deviation at about 20 K the fit is excellent. As a further test of the validity of the analysis it was felt essential to see if the temperature-dependent data alone showed any systematic departures from theory. Such systematic variations had been overlooked by authors who have previously used Fuchs's theory in the fitting of thickness dependences alone. That no such departure occurs in the present data is well illustrated in figure 8*a*. Here are shown the temperature dependent data for two samples, at the limits of the range in thickness, compared with theory. Clearly the data curves have the same form, the slight displacement reflecting the variation in C from sample to sample. Thus we can confidently state that both the temperature and thickness dependences of the resistivity of these films are dominated by grain-boundary scattering. This also confirms previous suggestions that gold films on mica are characterized by highly specular surface scattering. Our data suggest that r has a best value of 0.05 being certainly less than 0.1. This is equivalent, in the short mean free path, high temperature, limit (see Sambles & Elsom) to a specularity of greater than 0.65, probably nearer 0.85. It must, of course, be appreciated that the value of r is deduced on the basis of Soffer's theory which treats both surfaces of the film as equivalent. This is almost certainly not true and consequently r then represents an average value over both surfaces.

(*c*) *Films on* KBr *substrates*

(i) *Small-grained films*

As already discussed there are two distinct sets of data for $\langle 100 \rangle$ gold films on KBr. One set is distinguished from the other by a different growth behaviour and consequently different grain-boundary scattering. We shall consider first the set of data with the lower resistivity ratios, that is higher degree of grain-boundary scattering. The residual resistances of these films are well fitted by the above theory with again $r < 0.2$ and $\rho_i < 0.04$ nΩ m, the best fit being obtained with $r = 0.1$, $\rho_i \approx 0.02$ nΩ m (see figure 5) and corresponding values for β of 0.023 μm^{-1} and t_0 of 8.7 μm. These latter two parameters, combined with a C of 0.5 give a D_∞-value of 4.3 μm and an R_g-value of 0.10. As expected the R_g-value for the non-double-positioned $\langle 100 \rangle$ films is substantially less than that for the $\langle 111 \rangle$ films and also less than for the polycrystalline overlayer. Once again it appears that the thin-film resistivity is dominated by grain-boundary scattering.

Adopting then the same procedure as for mica we show in figure 7*b* a graph of $\rho/\rho_{g\infty}$ against

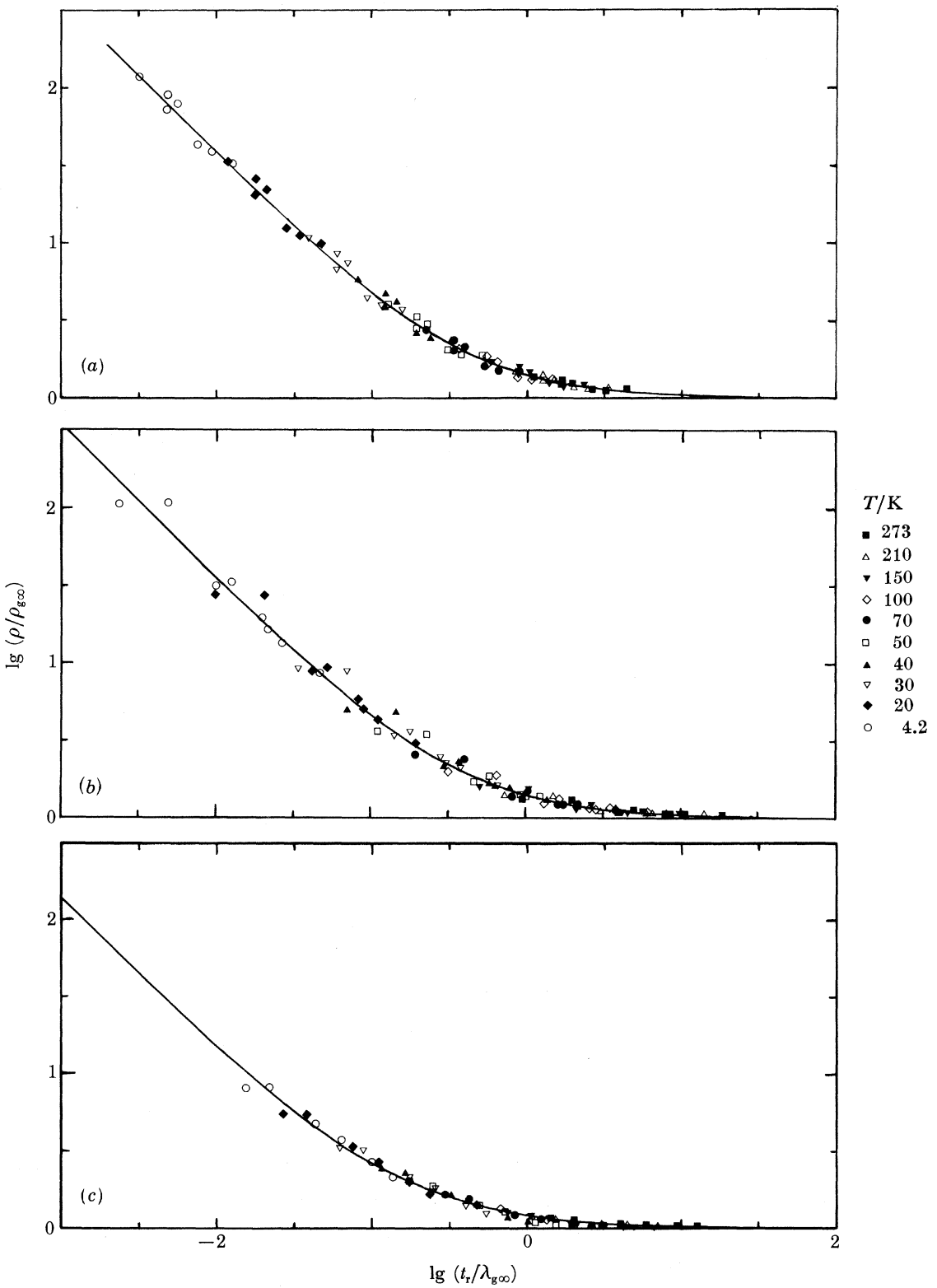

For description, see opposite.

PHILOSOPHICAL TRANSACTIONS OF THE ROYAL SOCIETY A MATHEMATICAL, PHYSICAL & ENGINEERING SCIENCES

$t_r/\lambda_{g\infty}$ for the same parameters as for figure 5. These provide, once again, an excellent fit over the whole temperature range. The same parameters were also used to produce the theoretical curves of figure 3*b*. These figures show a much greater spread in the data than the equivalent set for mica. This is attributed to the less well defined growth and the greater granularity of these ⟨100⟩ films.

Notwithstanding this scatter in the data the unislandized films fit the theory well, with similar parameters to those for the mica samples. Furthermore the temperature-dependent plots, as illustrated by samples from both ends of the thickness range (see figure 8*b*), also accord well (with slight shifts in C) with the theory. This shows, as for gold on mica, that surface scattering is almost negligible, the resistivity being dominated by grain-boundary scattering. In this case with $r \approx 0.1$ we may deduce an equivalent Fuchs specularity, in the high temperature limit, of *ca.* 0.65.

(ii) *Large-grained samples*

These very good quality films produced in an identical fashion to the other films on KBr presented several serious problems. The first lay in finding an explanation for the high r.r.rs compared with those of the other KBr samples. Scanning electron micrographs showed clearly that the morphology of these films was quite different to the low r.r.r. films, this being attributed to a different batch of KBr substrates of much higher quality, producing a different density of nucleation sites and correspondingly better epitaxial growth. A satisfactory explanation for the growth difference having been obtained, the r.r.r. difference is interpreted as being caused merely by this latter set having very large grains. The scanning micrographs show very few grain boundaries, leading to the proposition that the resistivity of these films will be dominated by either defect or surface scattering, rather than grain-boundary scattering. Nevertheless in view of the success in explaining the other sets of data using grain-boundary scattering theory with a small amount of surface scattering we initially adopted the same approach to these samples. With then, very similar parameters to those used for the first set of KBr samples, apart from the grain size, we obtained a good fit to the residual data as shown in figure 5. The same parameters produced a fit to the data over the whole range, in the form $\rho/\rho_{g\infty}$ against $t_r/\lambda_{g\infty}$ as shown in figure 7*c*. Here we fixed ρ_i as 0.020 nΩ m, the same as for the other KBr samples, the fit being very insensitive to this parameter. The other parameters used were again $r = 0.1$, as for the low r.r.r. samples, but $\beta = 0.16\ \mu m^{-1}$ and $t_0 = 0.41\ \mu m$. Since we do not know C, it makes it difficult to estimate the R_g-value. If, however, we take an R_g-value of 0.10 as for the low r.r.r. KBr samples, we find a C-value of 1.75 with a D_∞ of 0.71 μm, both of which are far too small. On the other hand if we guess a C-value of 20 we find D_∞ is 8 μm, but R_g is 0.56, which although of comparable value with that for mica, is nevertheless much higher than for the other KBr films. This suggests that the theory is not appropriate for this high quality set of films. Further, close inspection of figure 7*c* shows that at high temperatures the thick samples show a systematic deviation below the theoretical curve. This is particularly well illustrated in figure 8*c* where we plot $\rho/\rho_{g\infty}$ against $t_r/\lambda_{g\infty}$ for

FIGURE 7. Plot of $\rho/\rho_{g\infty}$ against $t_r/\lambda_{g\infty}$. Full lines are theoretical curves, $t_m = t_r$ being assumed, for (*a*) ⟨111⟩ gold on mica substrates, $r = 0.05$, $\rho_i = 0.020$ nΩ m, $\beta = 0.03\ \mu m^{-1}$, $t_0 = 8.7$ μm; (*b*) ⟨100⟩ gold on KBr substrates, small grains, $r = 0.1$, $\rho_i = 0.020$ nΩ m, $\beta = 0.023\ \mu m^{-1}$, $t_0 = 8.7$ μm; (*c*) ⟨100⟩ gold on KBr substrates, large grains, $r = 0.1$, $\rho_i = 0.020$ nΩ m, $\beta = 0.16\ \mu m^{-1}$, $t_0 = 0.41$ μm.

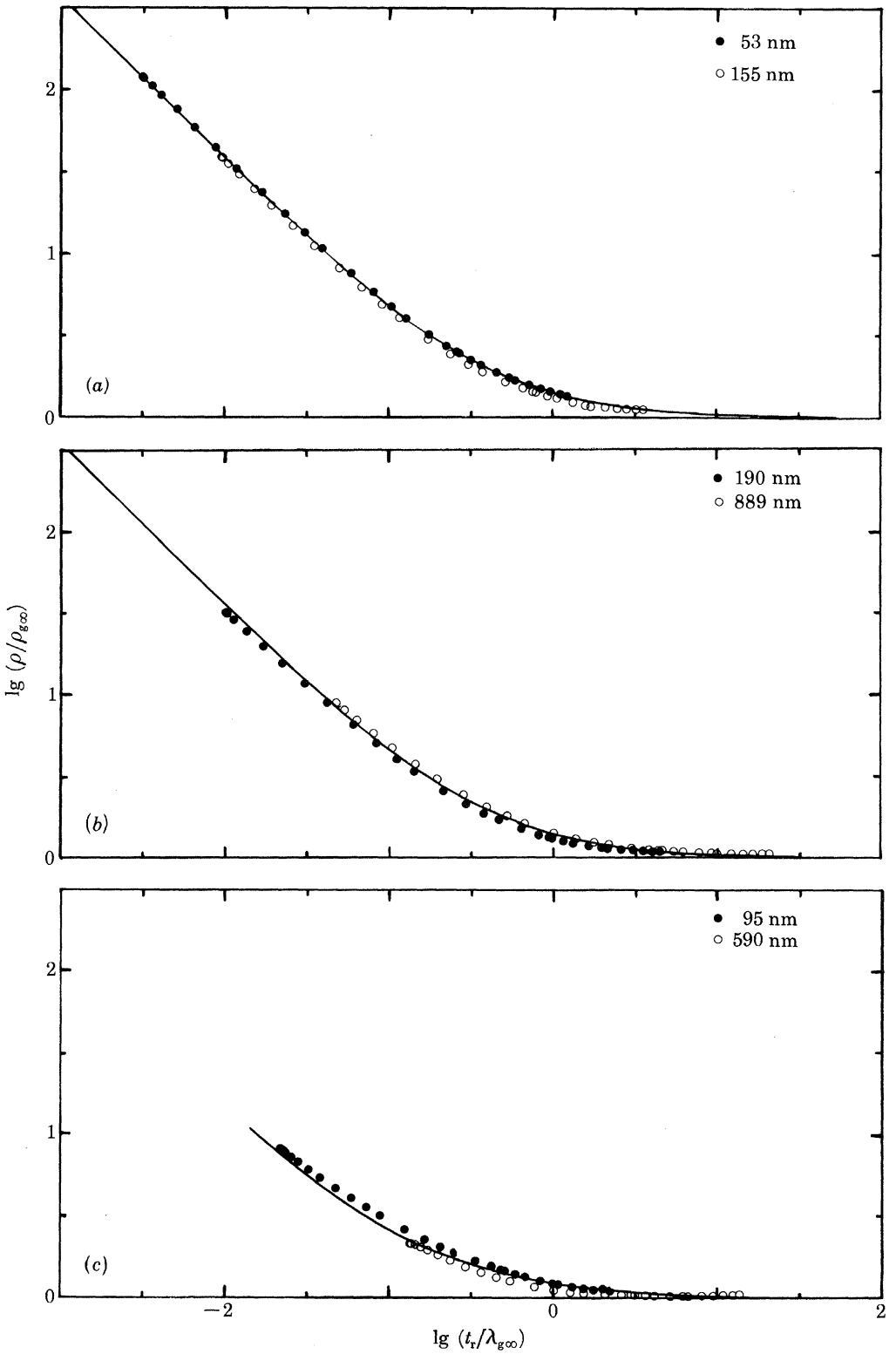

For description, see opposite.

PHILOSOPHICAL TRANSACTIONS OF THE ROYAL SOCIETY A MATHEMATICAL, PHYSICAL & ENGINEERING SCIENCES

the thickest and one of the thinner samples of this set. A clear systematic trend is seen in the thickest sample which implies very strongly that the theory is not applicable in this case. Furthermore, inspection of figure 4*c* shows a systematic deviation of the temperature dependence of the resistivity from theory with decrease in thickness.

Thus we tried the other approach, of removing grain-boundary scattering altogether (the grains were clearly very large) and trying to explain the data using surface scattering theory alone. The electron diffraction patterns and the high resolution micrographs suggested that these films were covered by a thin layer of *ca.* 10 nm diameter randomly oriented islands. How these islands are coupled electrically to the underlying gold layer is not known but it is possible that they merely make the surface appear rough, giving it a high r. The attempt at a fit to the data with the use of a high r-value worked extremely well for the residual resistivity with an alarmingly high r-value of 7.5. (Note that, for this very high value of r, Fuchs's theory will

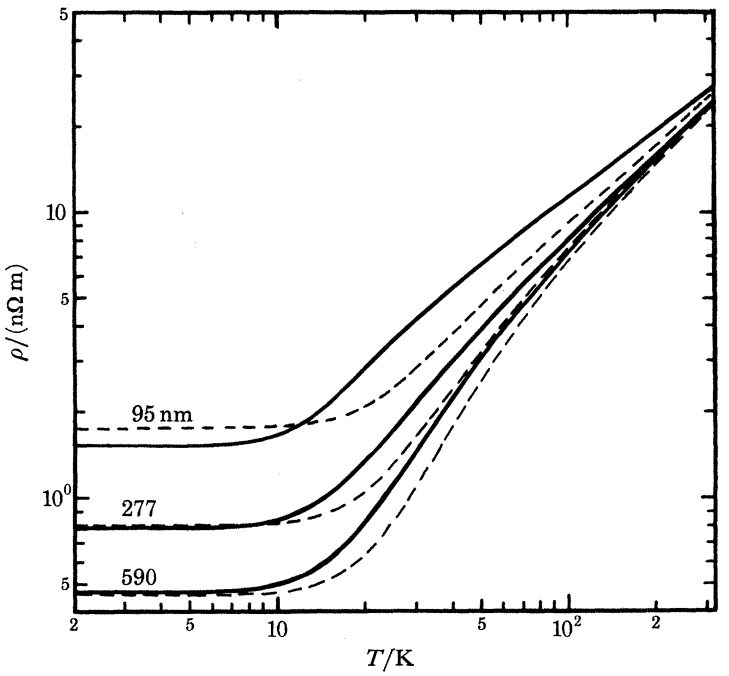

FIGURE 9. Resistivity against temperature for a few of the large-grained ⟨100⟩ films compared with a set of theoretical curves based on Soffer's surface scattering theory with an r of 7.5. The theory and experiment are made to be the same at 3 K. (See figure 5.)

give almost the same predictions with $p_F = 0$.) Using this r-value and Soffer's theory alone we produced the curves shown in figure 9 where it is transparently obvious that the predictions of this theory are wildly different to the observed results. Thus we note that, while these samples probably have little grain-boundary and very limited surface scattering, nevertheless their resistivity markedly increases with decrease in thickness. Furthermore, since the grain-boundary scattering approach gives a reasonable approximation we were forced to conclude that the

FIGURE 8. Plot of $\rho/\rho_{g\infty}$ against $t_r/\lambda_{g\infty}$ as a function of temperature. Full lines are theoretical curves with the same parameters as figure 7, $t_m = t_r$ being assumed, for (*a*) ⟨111⟩ gold on mica substrates; (*b*) ⟨100⟩ gold on KBr substrates, small grains; (*c*) ⟨100⟩ gold on KBr substrates, large grains.

PHILOSOPHICAL TRANSACTIONS OF THE ROYAL SOCIETY A MATHEMATICAL, PHYSICAL & ENGINEERING SCIENCES

scattering mechanism was a bulk- rather than surface-allied phenomena being almost certainly defect dominated. Epitaxial films of this nature will inevitably have substantial amounts of strain due to mismatch of the lattice parameters of the substrate and the gold. Normally this is relieved with the formation of grain-boundaries. In these high resistivity ratio films there are few grain-boundaries and consequently there will be a high level of strain within the films. How this varies with thickness and in what way it affects the resistivity is not known. However, it is to be anticipated that as the film grows in thickness, away from the substrate, so the strain density will decrease and consequently the resistivity scattering will also decrease giving the behaviour recorded.

6. Conclusions

We have measured the temperature-dependent resistivity of thin epitaxial gold films over the range 2 to 300 K. The results obtained are, for the most part, interpretable in terms of grain-boundary scattering theory. By modelling the grain size as a function of thickness we have produced theoretical comparisons with our data, obtaining for $\langle 111 \rangle$ films on mica an r of 0.05 and, for $\langle 100 \rangle$ films on KBr an r of *ca.* 0.1. These low values of r are equivalent, with a λ_e of 0.5 nm, to r.m.s. surface roughnesses of 0.025 and 0.05 nm respectively.

For the mica substrates this very small amount of surface roughness corresponds to only one atom in 14 being displaced from the equilibrium surface of the $\langle 111 \rangle$ films, while for the $\langle 100 \rangle$ films there are about twice this number displaced. In terms of the equivalent Fuchs specularity parameter, which is only relevant in the limit $\lambda_\infty \ll t$, the results give $p_F \approx 0.85$ for the $\langle 111 \rangle$ films and $p_F \approx 0.65$ for the $\langle 100 \rangle$ films. These numbers are in broad agreement with other studies and confirm the very limited amount of diffuse surface scattering in gold films. In contrast the grain-boundary scattering in these films is extensive. For the $\langle 111 \rangle$ films, which are double-positioned, the grain-boundary scattering is very significant with a grain-boundary reflexion coefficient of 0.45. This illustrates the very high degree of violation of the lattice periodicity condition at these boundaries. For the small-grained $\langle 100 \rangle$ films no such double-positioned boundaries exist, and the grain-boundary reflexion coefficient is much smaller, being only 0.10. Interestingly, the thick polycrystalline films on mica had an average grain-boundary reflexion coefficient of *ca.* 0.15, lying between the two other values and remarkably close to the value deduced from earlier studies by using equation (13) rather than (2).

Another set of $\langle 100 \rangle$ films on better quality KBr substrates were produced with very large grains and correspondingly high r.r.rs. These samples did not conform well to either Soffer's surface scattering theory or the grain-boundary scattering model. It is thought that their resistivities are dominated by defect scattering, the concentration of defects decreasing in a reasonably monotonic way with increase in thickness.

Considering the whole of this field of study in the light of the present results we can make several conclusions. Firstly, the surface scattering of gold is largely specular, as had been previously suggested, with a r.m.s. surface roughness of about 0.05 nm. Secondly, like previous studies we have found that the resistivity varies approximately as the inverse of the film thickness; this is well explained by grain-boundary scattering theory. Often in the past, because of the similar nature of equations (2) and (13), grain-boundary scattering has been misinterpreted as surface scattering. Thirdly, we find that, in general, the resistivity of gold films is almost always dominated by grain-boundary scattering. This is well illustrated by the many studies that record a 'ρ_∞' substantially higher than the accepted value. Fourthly, we note that this

study has shown, in relation to other studies, the *absolute necessity* of using both electron microscopy and electron diffraction to characterize as fully as possible the morphology of the films studied. This is best exemplified by the ⟨111⟩ films of gold on mica where three distinct growth regions are found. Any attempt to analyse the data from all these films with the use of one model will inevitably be erroneous.

Thus we see that this study has not only succeeded in its initial aim of largely clarifying the roles of surface and grain-boundary scattering in gold films, but it has also shown the necessity for simultaneous morphological studies of these films. We hope that henceforth all research in this area will incorporate a full characterization of the structure of the films before attempts are made to correlate any specific theory to the resistivity data and that consequently some of the dubious conclusions deduced in the past will not be perpetrated in the future.

J.R.S. acknowledges the Science Research Council for providing funds to purchase the instrumentation used in the resistivity measurements. The authors also wish to thank Dr R. M. Hooper of the Engineering Science Department for help in producing the electron micrographs and acknowledge the support of Dr J. E. Cousins.

References

Abelès, F. & Nguyen Van, V. 1970 *J. Physiol., Paris* C 1, 79–84.
Abelès, F. & Thèye, M. L. 1963 *Physics Lett.* **4**, 348–349.
Adamov, M., Perovic, B. & Nenadovic, T. 1974 *Thin Solid Films* **24**, 89–100.
von Bassewitz, A. & von Minnigerode, G. 1964 *Z. Phys.* **181**, 368–390.
Broquet, P. & Nguyen Van, V. 1967 *Surf. Sci.* **6**, 98–114.
Chauvineau, J.-P. & Croce, P. 1968 *C.r. hebd. Séanc. Acad. Sci., Paris* **266**, 1622–1624.
Chauvineau, J.-P. & Pariset, C. 1973 *Surf. Sci.* **36**, 155–172.
Chopra, K. L. & Bobb, L. C. 1964 *Acta metall.* **12**, 807–811.
Chopra, K. L., Bobb, L. C. & Francombe, M. H. 1963 *J. appl. Phys.* **34**, 1699–1702.
Chopra, K. L. & Randlett, M. R. 1967 *J. appl. Phys.* **38**, 3144–3147.
Cornely, R. M. & Ali, T. A. 1978 *J. appl. Phys.* **49**, 4094–4097.
Elsom, K. C. & Sambles, J. R. 1981 *J. Phys.* F **11**, 647–656.
Ennos, A. E. 1957 *Br. J. appl. Phys.* **8**, 113–117.
Fuchs, K. 1938 *Proc. Camb. phil. Soc.* **34**, 100–108.
Gillham, E. J., Preston, J. S. & Williams, B. E. 1955 *Phil. Mag.* **46**, 1051–1068.
Golmayo, D. & Sacedon, J. L. 1976*a* *Thin Solid Films* **35**, 137–141.
Golmayo, D. & Sacedon, J. L. 1976*b* *Thin Solid Films* **35**, 143–147.
Heras, J. M. & Mola, E. E. 1976 *Thin Solid Films* **35**, 75–82.
Hubin, M. & Gouault, J. 1972 *C.r. hebd. Séanc. Acad. Sci., Paris* **275**, 195–198.
Hubin, M. & Gouault, J. 1974 *Thin Solid Films* **24**, 311–331.
Jacobs, J. T., Birtcher, R. C. & Peacock, R. N. 1969 *J. Vac. Sci. Technol.* **3**, 339–342.
Kadereit, H. G. 1967 *Thin Solid Films* **1**, 109–130.
Kaveh, M. & Wiser, N. 1980*a* *Phys. Rev.* B **21**, 2278–2290.
Kaveh, M. & Wiser, N. 1980*b* *Phys. Rev.* B **21**, 2291–2308.
Lucas, M. S. P. 1964 *Appl. Phys. Lett.* **4**, 73–74.
Lucas, M. S. P. 1971 *Thin Solid Films* **7**, 435–444.
MacDonald, A. H. 1980 *Phys. Rev. Lett.* **44**, 489–493.
Matula, R. A. 1979 *J. phys. chem. Ref. Data* **8**, 1147–1298.
Mayadas, A. F., Henry G. R. & Shatzkes, M. 1972 *Appl. Phys. Lett.* **20**, 417–419.
Mayadas, A. F. & Shatzkes, M. 1970 *Phys. Rev.* B **1**, 1382–1389.
Mayadas, A. F., Shatzkes, M. & Janak, J. F. 1969 *Appl. Phys. Lett.* **14**, 345–347.
Meaden, G. T. 1966 *Electrical resistance of metals.* London: Heywood.
Meyer, D. T. 1968 *Thin Solid Films* **2**, 27–42.
Namba, Y. 1968 *J. appl. Phys.* **39**, 6117–6118.
Reale, C. 1970 *Acta phys. Pol.* A **37**, 3–7.
Sambles, J. R. & Elsom, K. C. 1980 *J. Phys.* F **10**, 1487–1494.

PHILOSOPHICAL TRANSACTIONS OF THE ROYAL SOCIETY A MATHEMATICAL, PHYSICAL & ENGINEERING SCIENCES

Sambles, J. R., Elsom, K. C. & Jarvis, D. J. 1979 *Solid St. Commun.* **32**, 997–1000.
Sambles, J. R., Elsom, K. C. & Sharp-Dent, G. 1981 *J. Phys.* F **11**, 1075–1092.
Soffer, S. B. 1967 *J. appl. Phys.* **38**, 1710–1715.
Tellier, C. R. & Tosser, A. J. 1976 *Thin Solid Films* **37**, 207–214.
Volger, J. 1950 *Phys. Rev.* **79**, 1023–1024.
Ziman, J. M. 1960 *Electrons and phonons*. Oxford University Press.

PHILOSOPHICAL TRANSACTIONS OF THE ROYAL SOCIETY A MATHEMATICAL, PHYSICAL & ENGINEERING SCIENCES

PHILOSOPHICAL TRANSACTIONS OF THE ROYAL SOCIETY A MATHEMATICAL, PHYSICAL & ENGINEERING SCIENCES

FIGURE 1. (*a*) Reflexion electron diffraction pattern (40 kV) from a high quality ⟨111⟩ gold film on mica. Note the long 'streaks' and double positioning. (*b*) Reflexion electron diffraction pattern (40 kV) from a thick ⟨111⟩ gold film with a polycrystalline overlayer. (*c*) Scanning electron micrograph of a just-conducting ⟨111⟩ film on mica. Note the channelled structure. (*d*) Scanning electron micrograph of a flat ⟨111⟩ film on mica showing grain size. (*e*) Scanning electron micrograph of a thick ⟨111⟩ film on mica showing very rough overlayer.

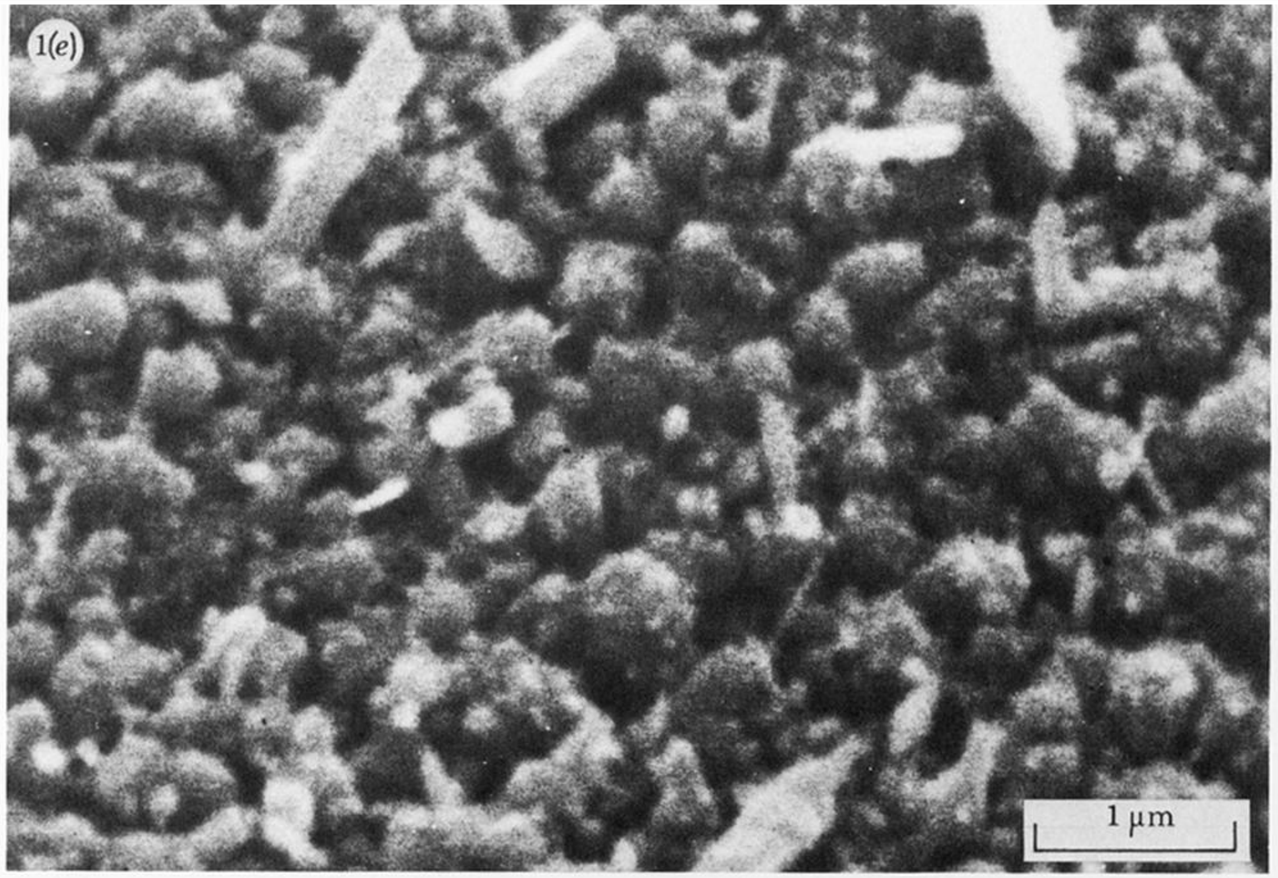

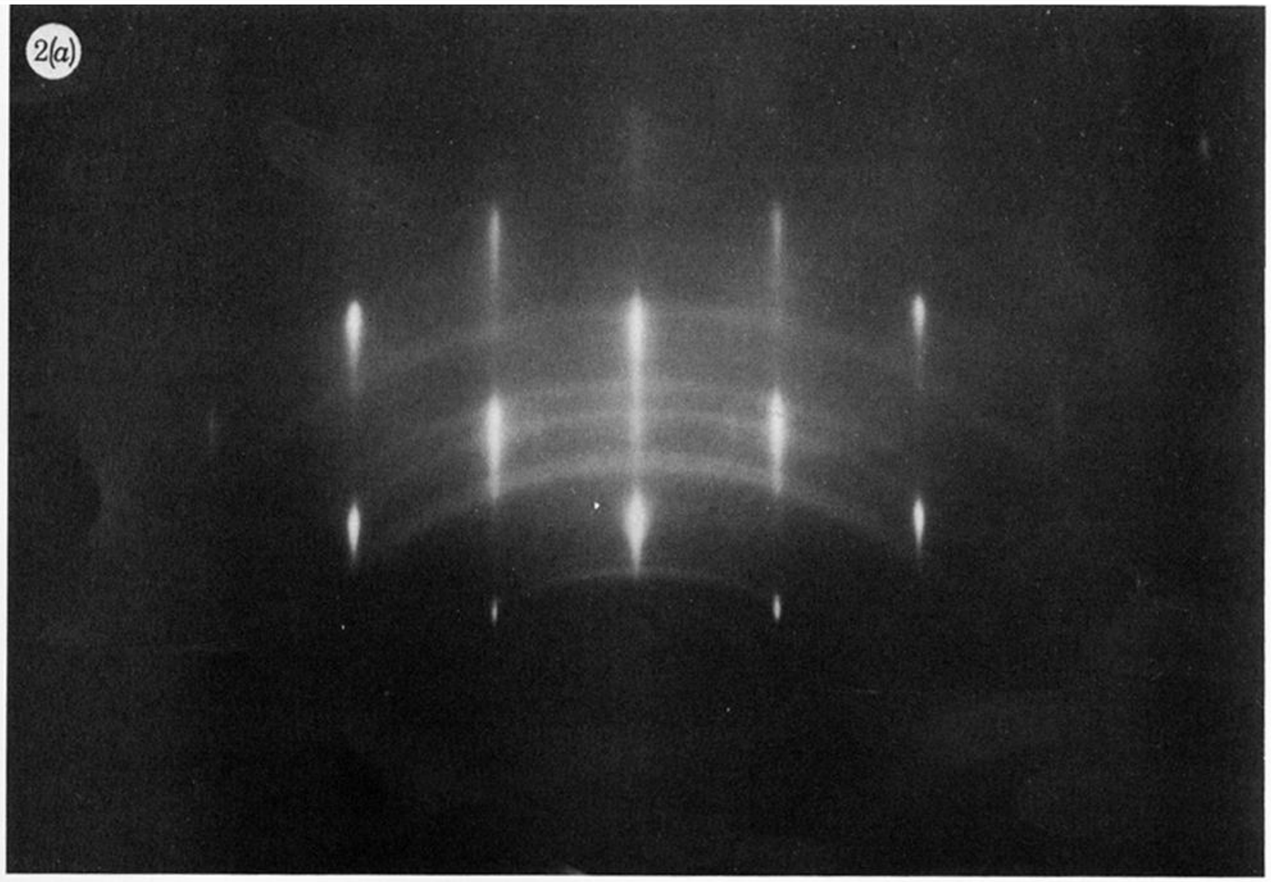

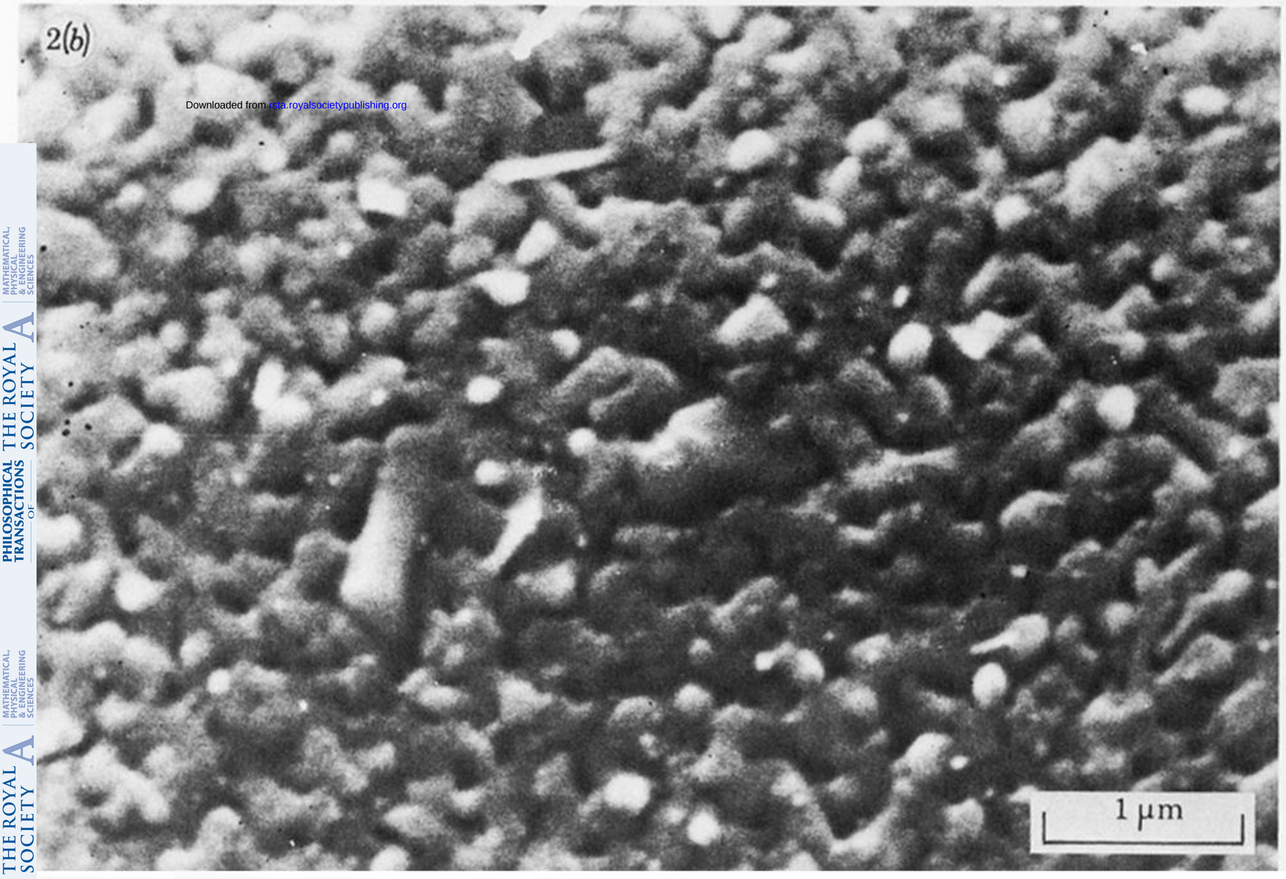

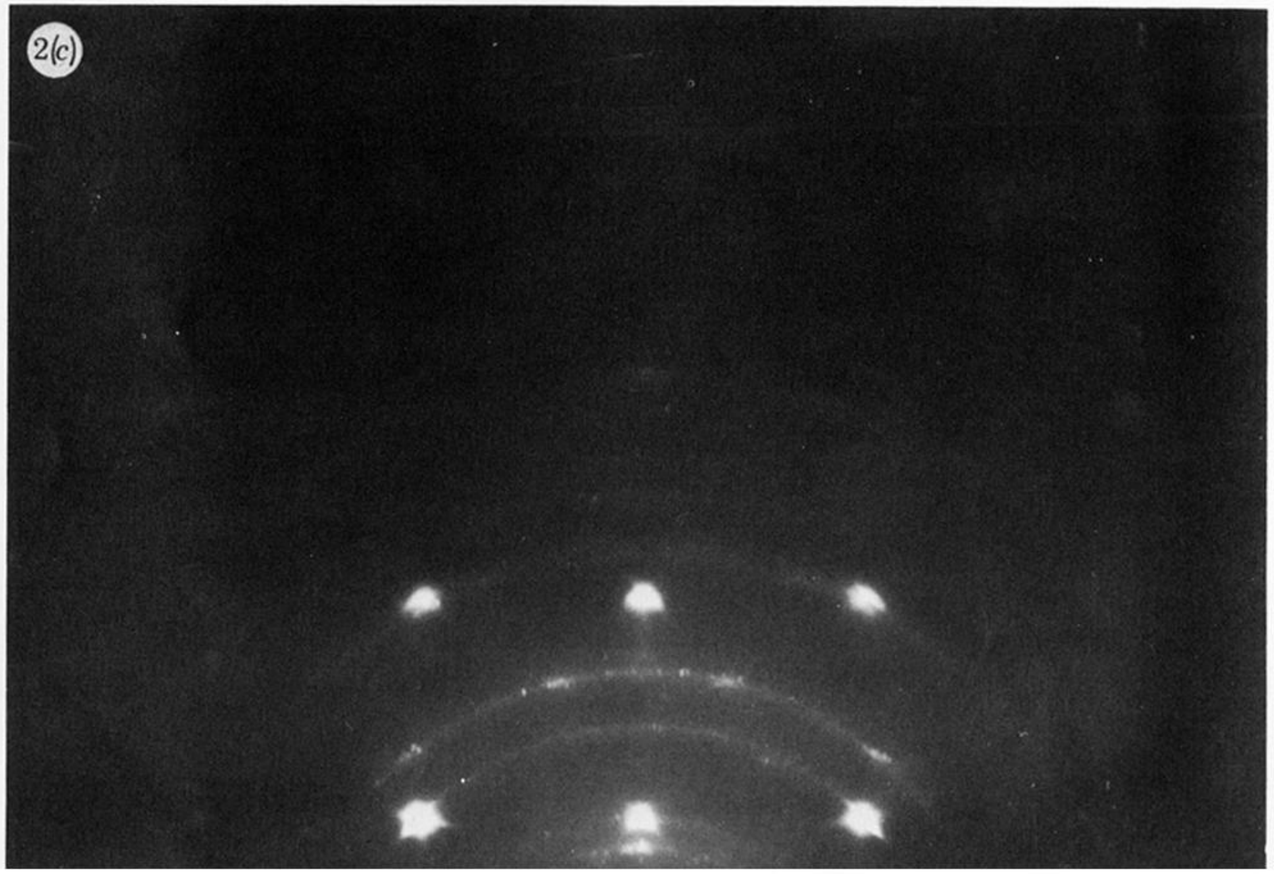

FIGURE 2. (*a*) Reflexion electron diffraction pattern (40 kV) from a ⟨100⟩ gold film on KBr showing a mixture of rings from a thin overlayer plus short 'streaks' indicative of a stepped surface. (*b*) Scanning electron micrograph of a low r.r.r. ⟨100⟩ gold film on KBr showing the grain size. (*c*) Reflexion electron diffraction pattern (40 kV) from a ⟨100⟩ gold film showing faceted nature of grains as illustrated by diffraction 'stars'.

PHILOSOPHICAL TRANSACTIONS OF THE ROYAL SOCIETY A MATHEMATICAL, PHYSICAL & ENGINEERING SCIENCES